DESIGN REPORT

THE FERMILAB HIGH-INTENSITY

ANTIPROTON SOURCE

FERMI NATIONAL ACCELERATOR LABORATORY

October, 1979

Participants in the Study

B. Brown, D. Cline, F. Cole, E. Colton, T. Collins, E. Crosbie, N. Dikansky, T. Fields, A. Garren, E. Gray, J. Griffin, W. Herrmannsfeldt, R. Huson, D. Johnson, W. Kells. G. Lambertson, C. Leemann, A. Lennox, J. MacLachlan, P. McIntyre, I. Meshkov, G. Michelassi, F. Mills, Y. Miyahara, D. Moffett, J. Nicholls, L. Oleksiuk, I. Orosz, V. Parkhomchuk, T. Rhoades, A. Ruggiero, J. Simpson, G. Silvestrov, L. Teng, and D. Young

Argonne National Laboratory

Fermi National Accelerator Laboratory

Institute of Nuclear Physics, Novosibirsk, USSR

Lawrence Berkeley Laboratory

University of Wisconsin

Contents

Abstract

A design study group has been developing a plan for achieving proton-antiproton collisions at a luminosity of 10^{30} cm^{-2} sec^{-1} in the Fermilab 1-TeV Superconducting Accelerator. In this report a design is presented that uses a Precooler ring, about Booster length, to collect and stochastically momentum-cool antiprotons produced by 80-GeV protons from the Fermilab Main Ring. When the circulating beam has been sufficiently cooled, it is transferred to the Electron Cooling Ring for accumulation and further cooling. Stochastic momentum cooling is very effective for high-energy, large momentum-spread beams, and electron cooling is most effective for relatively cool beams at low energy. Furthermore, electron cooling works equally well for transverse and longitudinal beam dimensions. The plan therefore exploits the relative advantages of both stochastic and electron cooling. A recent recognition that the stochastic-cooling process can be effectively iterated in steps separated by deceleration has resulted in placing modest demands on the Electron Cooling Ring and makes the attaining of the design goals substantially less dependent on large extrapolations of current experience. Approximately 5 hrs of antiproton collection time are required to achieve the luminosity goal. A beam of 10^{11} antiprotons in collision with 10^{11} protons/bunch will produce a luminosity of more than 10^{30} cm^{-2} sec^{-1}.

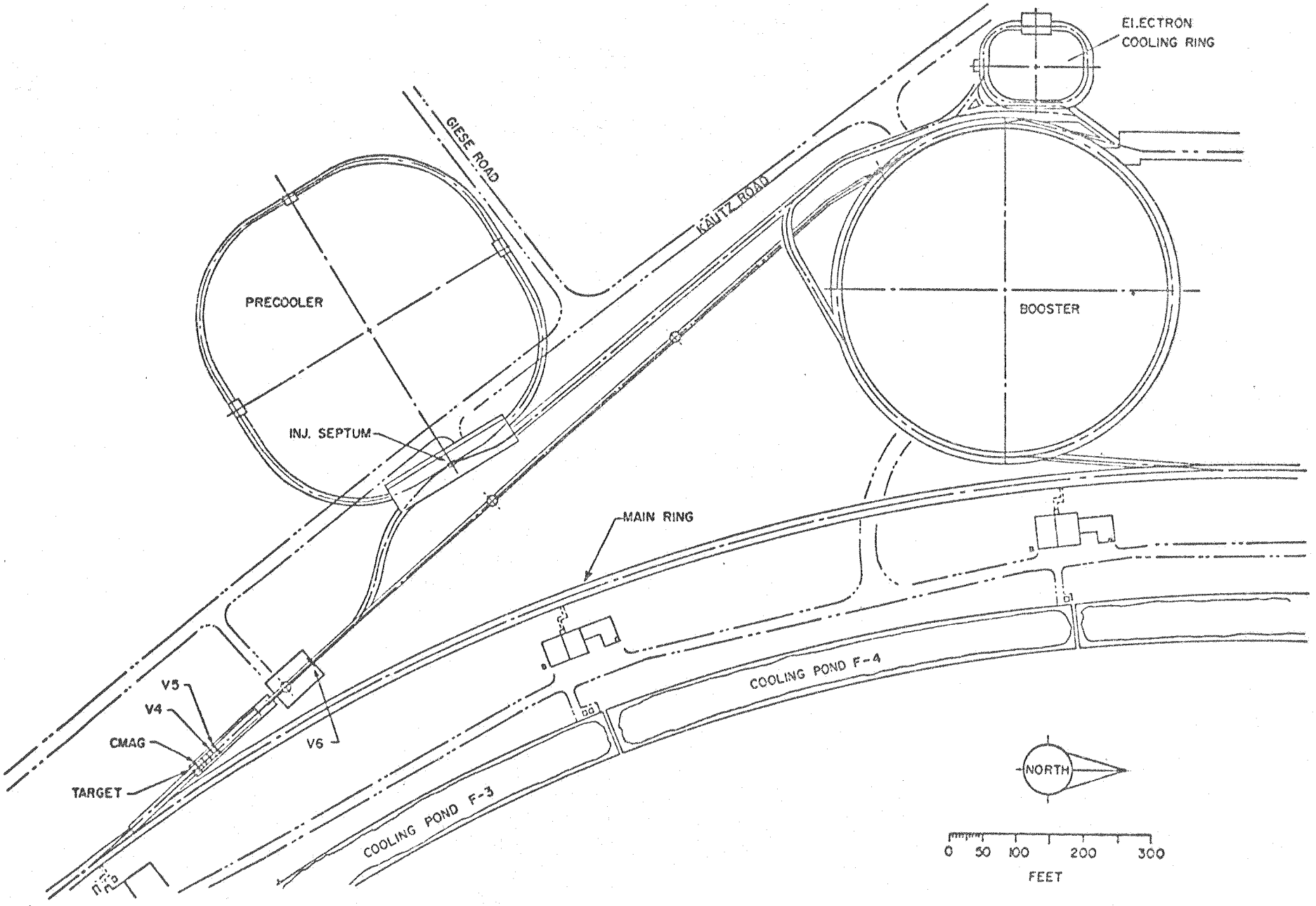

1-1 Layout of the High-Intensity Antiproton Source.

1. INTRODUCTION

1.1 Scope of the Report

This report describes the design of a high-intensity antiproton source to be constructed at the Fermi National Accelerator Laboratory. The centerpiece of this source is a Precooler, a storage ring and accelerator for cooling antiprotons. The Precooler is approximately the size of the Fermilab Booster accelerator. With this Precooler, the antiproton source will yield antiproton intensities that will produce antiproton-proton luminosities greater than 10^{30} cm^{-2} sec^{-1} at 2 TeV in the center of mass in the Energy Saver-Doubler superconducting accelerator already under construction at this Laboratory. The existing Electron Cooling Ring, in a modified and improved form will be a part of the plan. A layout of the plan showing the location of the Precooler is shown in Fig. 1-1.

The Precooler design discussed in this report is a magnet ring of 75.47 m average radius with four long straight sections, which are dispersion-free. There are rf systems for deceleration and acceleration. It is to be installed in its own tunnel south of the Booster, by the intersection of Kautz and Giese Roads, and connected to the Main Ring and Electron Cooling Ring by beam-transport tunnels.

It is the current plan to leave the Electron Cooling Ring in its present configuration and location. It will, however, be necessary to improve the facility, to upgrade some power-supply systems, and to add some shielding for the stacking of a beam of 10^{11} 200-MeV antiprotons.

1.2 Concept of the Precooler

The concept of colliding-beam experiments with antiprotons and protons at Fermilab was first proposed by Cline, McIntyre, Mills and Rubbia[1] in 1976. The system envisaged initially used electron cooling exclusively and would, it was estimated, produce a luminosity of 5×10^{28} cm^{-2} sec^{-1}. The electron cooling was to be accomplished in a 200-MeV storage ring. A research and development effort began in 1977 to build a small ring for tests of electron cooling. This ring is now virtually complete.

Further study, including a workshop in 1978,[2] has led to the belief that it would be possible to produce a luminosity greater than 10^{30} cm^{-2} sec^{-1}, far more useful for experiments. A general plan using a separate Precooler ring has several significant advantages. It now appears that it will be difficult to achieve the 50-msec cooling time in the existing Electron Cooling Ring needed to synchronize efficiently with the Booster cycle. It is possible to consider extending the straight sections of the Electron Cooling Ring to install more cooling

and thus shorten the cooling time, but there are severe difficulties in the accelerator lattice of such an extension.[3]

What is discussed here is therefore a plan to utilize the Precooler to capture 4.5-GeV antiprotons and momentum-cool them stochastically in several steps[4] as they are decelerated to 200 MeV. The 200-MeV beam is extracted then injected into the existing Electron Cooling Ring, where it is cooled further both in momentum and in betatron phase space. The sequence is repeated, stacking the antiproton beam in the Cooling Ring until approximately 10^{11} have been accumulated. This beam is then transferred back to the Precooler, accelerated to 8 GeV and injected into the Main Ring and Superconducting Ring for acceleration to 1 TeV.

1.3 The Development Effort

In late 1978, an informal design study group began to meet regularly at Fermilab in order to develop a plan for producing high-luminosity $\bar{p}p$ collisions in the Energy Saver-Doubler. Participants in this design study are from Fermilab, ANL, LBL, and the University of Wisconsin. The study group has been part of the larger collaborative research and development effort among the above institutions, plus the Institute of Nuclear Physics, Novosibirsk to develop $\bar{p}p$ capabilities at Fermilab.

At first the group worked to establish a better understanding of appropriate accelerator physics and technology, including questions regarding fundamental limits of the performance of various systems. It has gone on to analyze quantitatively various suggested schemes from the standpoint of technical feasibility and practical performance.

This report describes a specific design. This design is regarded as a basis for proceeding with the more detailed design and construction of a high-luminosity $\bar{p}p$ colliding-beam system at Fermilab. Luminosity of greater than 10^{30} cm^{-2} sec^{-1} after a few hours of antiproton collection time should be possible with the scheme, provided that the performance of the techniques utilized can, in fact, be realized. Some of the important items are:

(i) Electron Cooling Ring Performance. The experimental data from Novosibirsk on electron cooling are incomplete and do not quite address the problems of cooling large-emittance beams and of accumulation. Recently, CERN has accomplished electron and stochastic cooling and it appears that the predictions of the theory are borne out by the experiments.

(ii) Main-Ring performance. The plan presented here requires Main-Ring charge redistribution. Although a preliminary experiment has been conducted[5] there is still work to be done in this area.

(iii) Similarly, experiments will be undertaken to investigate the assumption that large bunch charge (of order 10^{11} p/bunch) can be produced and stored in the Superconducting Ring.

(iv) $\bar{p}$ production targetry is a complicated part of the plan. Experiments need to be conducted to evaluate realizable proton beam quality and various target design options.

Currently a research and development program is being pursued to address these items. A major effort during 1980 will be directed toward experiments on the Electron Cooling Ring, both on electron cooling and stochastic cooling, on storing and rebunching proton beams in the Main Ring, and on the construction of an extraction and target system for 80-GeV protons. It is also a goal to acquire experience in handling low-intensity $\bar{p}$-beams by decelerating them in the Booster accelerator to 200 MeV and transporting them to the Electron Cooling Ring for cooling and accumulation.

Obviously, the design will be refined as more detailed information is obtained, but the framework developed in the last year and described in this report is adequate to support the anticipated detailed development without fundamental changes in scope or concept.

References

[1] D. Cline et al., Proposal for Fermilab Expt. 492, 1976.
D. Cline, P. McIntyre, F. Mills, and C. Rubbia, Collecting Antiprotons in the Fermilab Booster and Very High Energy $\bar{p}$ Collisions. Fermilab Report TM-687, 1976.

[2] Proceedings of the Workshop on Producing High Luminosity, High Energy Proton-Antiporton Collisions, March 27-31, 1978. Fermilab and Lawrence Berkeley Laboratory Report LBL-7574.

[3] D. E. Johnson , New Thoughts on the Extended Electron Cooling Ring Lattice, Fermilab $\bar{p}$ Note 21, Aug. 1979.
D. E. Johnson, Fast Electron Cooling and an Expanded Electron Cooling Ring, Fermilab $\bar{p}$ Note 41, Sept. 1979.
A. Ruggiero, On the Effects of Inserting Long Cooling Regions, Fermilab $\bar{p}$ Note 49, Sept. 1979.

[4] W. P. Kells, Methods for Longitudinal Cooling by Large Factors in a $\bar{p}$ Precooler Ring, Fermilab $\bar{p}$ Note 43, October 1979.

[5] J. E. Griffin and F. E. Mills, Proc. of the 1979 Particle Accelerator Conference, IEEE Trans. Nucl. Sci., NS-26, No. 3, Jun. 1979, p. 3589.

2. SYSTEM PERFORMANCE

2.1 The Sequence of $\bar{p}$ Collection

The sequence of steps to collect the required number of antiprotons is outlined here and presented in more detail in Section 3 of this report.

1. Approximately two-thirds of the Main-Ring circumference is loaded by the Booster for acceleration. The Main Ring accelerates 1.8×10^{13} protons to an energy of 80 GeV, then flat-tops.

2. The charge is redistributed in the Main Ring by rf manipulation to occupy approximately 1/13 the circumference (one Precooler length). All finer time structure is lost in this process.

3. The protons are extracted in a single turn and targeted on a $\bar{p}$ production target.

4. Antiprotons are collected in a large-aperture Precooler ring, of approximately Booster circumference, at 4.5-GeV kinetic energy in a transverse emittance of 4.8π mm-mrad in each plane and momentum spread $\pm$ 2%. The beam is stochastically momentum cooled by a factor of about a hundred in several seconds.[1] Cooling takes place in three or four steps, each 1 to 2 seconds cooling followed by some deceleration to re-establish phase mixing.

5. The cooled beam is decelerated to 200 MeV. Depending on the stochastic cooling realized, the beam will be bunched on either the first or second harmonic to reduce the bunch length down to the circumference of the Electron Cooling Ring, then transferred to that ring. If it is necessary, bunches will be transferred and cooled sequentially.

6. The antiprotons are bunched on a low harmonic ($h \approx 6$ to 12) in the Electron Cooling Ring, then individual bunches are transferred to the Precooler ring at harmonic number 21, accelerated to 8 GeV and injected into the Main Ring, accelerated, then transferred into the Superconducting Ring in the reverse direction.

7. Protons are accelerated in the conventional manner in the Main Ring and transferred into the Superconducting Ring. Both beams are simultaneously accelerated to collision energy.

2.2 System Parameters

Parameters of a system to carry out these indicated steps are summarized in Table 2-I.

Table 2-I System Performance Parameters

	Antiproton Production
Proton energy for production (E_p)	80 GeV
Protons per MR cycle	1.8×10^{13}
MR cycle time	8 sec
Protons/sec	2.2×10^{12}
Antiproton energy (at collection)	4.5 GeV
$\bar{p}$ transverse acceptance at 4.5 GeV, horizontal	$4.8\pi \times 10^{-6}$ m-rad
$\bar{p}$ transverse acceptance at 4.5 GeV, vertical	$4.8\pi \times 10^{-6}$ m-rad
$\bar{p}$ momentum collection ($\Delta p/p$)	$\pm$ 2%
Invariant $\bar{p}$ cross section ($Ed^3\sigma/dp^3$)	0.8 mb/GeV^2
Total absorption cross section (σ_o)	33 mb
Number of $\bar{p}$'s per proton ($N_{\bar{p}}/N_p$)	3.2×10^{-6}
$N_{\bar{p}}$/sec.	$7.0 \times 10^{+6}$
$N_{\bar{p}}$/h (with 80% efficiency factor)	2.0×10^{10}

2.3 Luminosity of $\bar{p}p$ Collisions

A scheme to produce a luminosity of 5×10^{28} cm^{-2} sec^{-1} was developed some time ago.[2] Provided the present Main-Ring proton intensity can be rebunched to approximately 10^{11} p/bunch (10 times the present bunch density) the collision of one such bunch with a single bunch of 6×10^9 antiprotons will yield a luminosity of 5×10^{28}. Development of higher-luminosity schemes primarily depends upon the use of more bunches and more antiprotons. Table 2-II lists a comparison of collision parameters for the scheme presented here and of the CERN project now under construction.

Table 2-II Luminosity Comparison

	Fermilab	CERN
Energy (GeV)	1000	270
Number of Protons (N_p)	1.2×10^{12}	6×10^{11}
Number of antiprotons ($N_{\bar{p}}$)	10^{11} (5 h)	6×10^{11} (24 h)
Number of bunches	~ 12	6
Low beta at interaction $\beta^* = \sqrt{\beta_x \beta_y}$ m)	1.5	2.2
Proton emittance, horizontal (m-rad)	$2.6\pi \times 10^{-8}$	$3.5\pi \times 10^{-8}$
Proton emittance, vertical (m-rad)	$2.6\pi \times 10^{-8}$	$3.5\pi \times 10^{-8}$
Antiproton emittance, horizontal (m-rad)	$1.0\pi \times 10^{-8}$	$3.8\pi \times 10^{-8}$
Antiproton emittance, vertical (m-rad)	$1.0\pi \times 10^{-8}$	$1.9\pi \times 10^{-8}$
Luminosity (cm^{-2} sec^{-1})	$>10^{30}$	10^{30}
Bunch length (m)	1	-

In addition to collection of more antiprotons and more bunches, there are possible improvements to be gained in

luminosity lifetimes and magnitude by utilization of high-energy electron-cooling techniques[3] or transverse stochastic cooling. Such techniques are not, however, within the main thrust of this report.

References

[1] W. Kells, Methods for Longitudinal Cooling by Large Factors in a $\bar{p}$ Precooler Ring, Fermilab $\bar{p}$ Note 43, Oct. 1979.

[2] F. E. Mills and D. E. Young, A Scenario to Achieve a Luminosity of Approximately 5×10^{29} cm^{-2} sec^{-1} for $p\bar{p}$ Collisions in the Fermilab Energy Doubler, unpublished report, Nov. 1978.

[3] D. Cline et al., High Energy Electron Cooling to Improve the Luminosity and Lifetime in Colliding Beam Machines, SLAC Pub 2278, March 1979.

3. ANTIPROTON PRODUCTION AND TRANSPORT

3.1 Requirements and General Layout

Here we summarize some considerations and parameters involved in the production and collection of antiprotons. The overall goal is to maximize the antiproton yield by appropriate design of the extracted beam, the p beam line, the production target, and the $\bar{p}$ beam line. The principal difficulties in achieving this goal arise from the very small spot size (< 1 mm diam.) that is needed to obtain high $\bar{p}$ source brightness and the resulting stringent conditions on beam optics and target heating and from the necessity to produce an antiproton beam of length appropriate to fit in the Precooler.

The basic parameters affecting the yield are taken to have the values given in Table 3-I.

Table 3-I Antiproton Production Parameters

Proton energy	80 GeV
Antiproton energy	4.5 GeV
Antiproton emittance accepted by Precooler	$4.8\pi \times 4.8\pi$ mm-mrad
Proton beam emittance	0.15π mm mrad
Momentum Acceptance of Precooler	±2%

The 80-GeV proton beam will be rebunched in the Main Ring to fit in a total length corresponding to the Precooler circumference, extracted at F17 and transported to the antiproton production target located in the Target Vault. The 4.5-GeV antiproton beam will then be transported to the Precooler. An overall layout of the system was shown in Fig. 1-1.

3.2 Operation of the Main-Ring Beam for High-Intensity Extraction

In order to maximize the $\bar{p}$ intensity in a Booster-size Precooler, it will be advantageous to do single-turn injection of $\bar{p}$'s. Maximum intensity will be obtained if the largest possible quantity of Main-Ring beam is placed on the $\bar{p}$ target during a period slightly less than the revolution period in the Precooler. Because the Main-Ring beam is initially distributed uniformly around at least a large fracton of the ring, redistribution of the beam prior to extraction will be required.

Recent measurement of the longitudinal emittance of individual Main Ring bunches at 100 GeV indicate emittances of about 0.2 eV-sec with 10^{10} protons per bunch corresponding to 213 eV-sec for the entire ring. If this emittance is coalesced into a 1.6-μsec time slot, the energy spread will be 133 MeV and the fractional energy (or momentum) spread at 80 GeV will be 1.66×10^{-3}, a momentum spread easily contained in the Main-Ring aperture.

The Main-Ring beam could be coalesced into the 1.6-μsec time slot using a first-harmonic rf cavity operating at 47.7 kHz; the voltage required would be approximately 50 kV. Such a cavity is not beyond question, but it would be a large and expensive device. Instead we will utilize a procedure by which a large fraction of the Main-Ring beam can be coalesced into a small azimuthal region just prior to extraction using only the existing Main-Ring rf system (53 MHz, h = 1113).

In order to coalesce protons from a wide range of azimuthal locations into a smaller region, charge from various parts of the ring must be advanced or retarded with respect to some location designated as synchronous. This can be accomplished if the central momentum of each bunch varies linearly with distance from this synchronous bunch. With such a distribution established and all rf buckets removed, the bunch distribution will coalesce to the azimuthal location of the synchronous bunch in a time that depends on the momentum deviation and the energy. Because of the momentum spread within each bunch, the synchronous bunch, as well as all the others, will debunch during this drift time, so the fraction of the ring into which beam can be coalesced depends on the individual-bunch momentum spread, as well as on the momentum deviation of the nonsynchronous bunches. The useful aperture of the Main Ring and the initial longitudinal beam emittance place limitations on the entire process.

Let the total energy spread within a single bunch just prior to removal of the rf constraint be ΔE_b. After removal of the rf, the bunch will spread during some drift time T_b into a time interval ΔT given by

$$\frac{\Delta T}{T_d} = \eta \frac{\Delta E_b}{E_s}, \tag{3.1}$$

where η is the momentum dispersion and E_s is the synchronous energy. If ΔT is a fraction F of a Main-Ring revolution period T_o, then the drift time T_d is

$$T_d = \frac{E_s \, F \, T_o}{\eta \, \Delta E_b}. \tag{3.2}$$

During the drift time (many turns), a synchronous bunch advances by an azimuthal angle θ given by

$$\theta = 2\pi \frac{T_d}{T_o}. \tag{3-3}$$

A bunch with its centroid removed from the synchronous energy by an energy deviation ΔE_d will gain or lose in azimuthal position by

$$\frac{\Delta\theta}{\theta} = \eta \frac{\Delta E_d}{E_s} \tag{3-4}$$

Then the total azimuthal angle gained or lost by a non-synchronous bunch during the drift time T_d is

$$\Delta\theta = 2\pi F \frac{\Delta E_d}{\Delta E_b} \text{ or } \frac{\Delta E_d}{\Delta E_b} = \frac{\Delta\theta}{2\pi F} \tag{3-5}$$

If the goal is to coalesce beam from 70% of the ring into an azimuthal length equal to that of the Precooler circumference, then $\Delta\theta$ becomes $\pm 0.7\pi$ and F is 1/13.25. This gives the required ratio of the deviation energy of those bunches farthest removed from the synchronous bunch to the internal energy spread of whichever bunch has the greatest spread

$$\frac{\Delta E_d}{\Delta E_b} = \frac{0.07\pi \times 13.25}{2\pi} = 4.64 \tag{3-6}$$

The procedure to relocate the beam is then as follows:

1 The Main Ring (h = 1113) is loaded with Booster batches (h = 84) in the normal manner and the beam is accelerated to 80 GeV, where the guide field is held constant for approximately 2 seconds. Only that fraction of the Main Ring that will be coalesced need be filled with Booster batches.

2. During the transition from ramp to constant field, the rf voltage is adjusted adiabatically to a level of 4 MV, yielding minimum bunch length and maximum momentum spread. This configuration is shown roughly to scale in Fig. 3-1a. The bucket height is 0.77 eV-sec or 257 MeV; the bunch width is initially 2.5 nsec.

3. The rf is switched to the unstable phase angle and the bunches are allowed to deform along the separatrix until the bunches have a (projected) bunch length of 3 nsec. The total bunch length in the bucket becomes 1 rad. This is shown in Fig. 3-1b.

4. The rf is switched back to the stable stationary-bucket phase angle and the bunches are allowed to rotate approximately one-quarter of a synchrotron oscillation, as shown in Fig. 3-1c. The synchrotron period is 4.2×10^{-3} sec, so this operation requires only a few milliseconds.

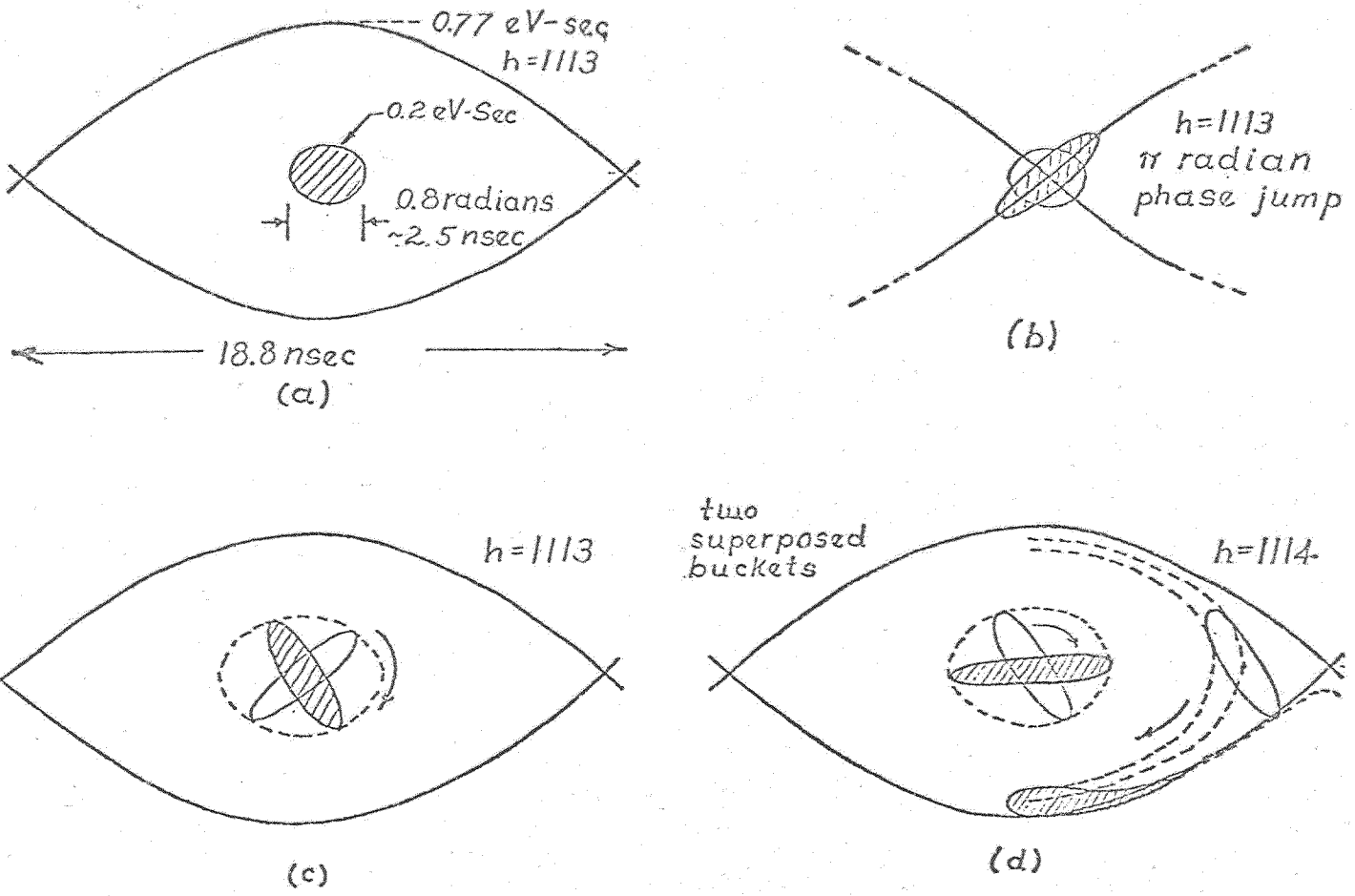

Fig. 3 - 1.a) 4 MV, h = 1113 bucket containing a matched bunch with emittance 0.2 eV-sec and bunch width 2.5 nsec. b) The same bucket as part (a) switched to the unstable phase angle. The bunch is allowed to distort along the separatrix until its width is 3 nsec. (3) The bucket switched back to stable position and the distorted bunch allowed to rotate about one quarter turn. (d) Superposition of two h = 1114, 4 MV buckets, one containing a centered bunch, the other containing a bunch displaced within the bucket to 0.7π radians. During the allowed drift time the bunches rotate to the positions shown.

5. The rf is switched to one harmonic number higher than the original frequency in a time short compared with a synchrotron period. During normal acceleration, the rf system is tuned over a frequency range of 290 kHz, so a frequency jump of one revolution frequency, 47.7 kHz, is well within the normal tuning range. The (h + 1) rf voltage is

$$V(t) = V_0 \sin (h + 1)\, \Omega_0\, t, \qquad (3\text{-}7)$$

where h is the original harmonic number and Ω_0 is the synchronous angular revolution frequency. The time of arrival of the k-th bunch at the effective accelerating gap location is then

$$t_k = k/f_{rf} = \frac{k}{h} T_0,$$

so the voltage seen by the k-th bunch immediately following reapplication of the rf voltage is

$$V_k = V_o \sin \frac{2\pi k}{h}. \qquad (3\text{-}8)$$

Since k ranges from zero to h, the voltage applied to the h bunch locations initially has the appearance of a voltage applied on the first harmonic. The important distinction between this ring voltage and a voltage at h = 1 is that the bunches are constrained to remain within a phase space defined by new buckets which have the same phase extent as the original buckets to within 0.1%.

Because of the one-unit difference between the number of buckets established at (h + 1) and the original number of bunch locations, one bunch will be centered in the new bucket and bunches to either side of the centered bunch will be progressively displaced within the buckets. The center of the k-th bunch is displaced from the center of its bucket by an angle S = 2π k/h (rf radians, $-556 \leq k \leq 556$). With the application of the (h + 1) rf voltage, the bunches begin to execute coherent synchrotron oscillations from these initial positions. The synchrotron motion is allowed to continue until bunches with small displacements have executed approximately 3/8 of one oscillation. This allows bunches with larger initial phase displacement, but lower synchrotron frequency to reach a high momentum deviation. This motion is shown in Fig. 3-1d for the centered bunch and for a bunch displaced from the center of the bucket by 2.2 rad (0.7π). The centered bunch rotates on the phase contour shown to a horizontal position with total momentum spread of 0.148 eV-sec (49.4 MeV). The centroid of the bunch with initial displacement of 0.7π radians moves approximately one-fourth of a turn to a displacement of 0.686 eV-sec (220 MeV). The lower edge of the displaced bunch moves on a contour very close to the separatrix, while the innermost boundary of the bunch moves along the contour shown to a displacement of 0.63 eV-sec (210 MeV). The momentum spread of the displaced bunch then becomes 0.14 eV-sec, about the same as that of the centered bunch. The ratio of bunch displacement to momentum spread is

4.64, which is just that which is required by Eq. (3-6). The momentum deviation distribution of bunches around the ring at the end of this short period of phase oscillation is shown in Fig. 3-2.

6. When the bunches reach the displacements described in Step 5, the rf is removed and the bunches are allowed to debunch and coalesce. The drift time given by Eq. (3-2) for this example is 0.93 sec.

Results of the first attempt at a relocation experiment are shown in Fig. 3-3, where two Booster batches separated by 180° in the Main Ring are shown coalescing to about one-eigth the azimuth in a period of approximately 2 sec. In this experiment the rf voltages and the bunch widths were not optimized.

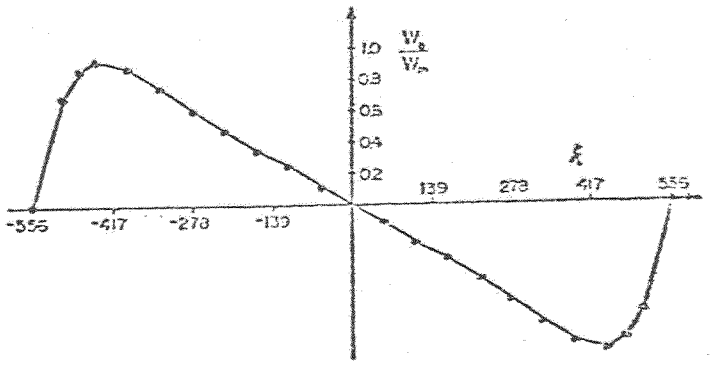

Fig. 3-2 Momentum deviation of bunches as a function of azimuthal position after 3/8 synchrotron period in buckets with harmonic number h + 1.

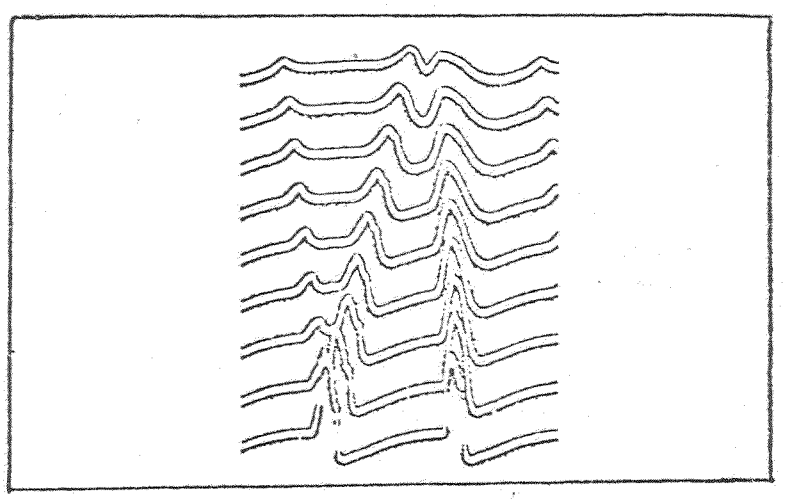

Fig. 3-3 Coalescence of two Booster batches originally separated by 180°. Time proceeds upward, traces separated by 0.2 sec.

3.3 Proton-Beam Transport System to the Target

The extracted 80-GeV proton beam element layout and beam transport system are shown in Fig. 3-4. Extraction takes place in straight section F17 where a septum magnet will be placed. A kicker magnet is located at C48, an odd number of quarter wavelengths upstream. Extraction will be in the vertical direction because less angular deflection is required to miss the following dipole than for horizontal extraction. The nearest Main-Ring dipole must have a special coil so that the beam pipe can pass next to the magnet steel, under the end loop.

The extracted beam is pitched flat 19 in. above normal orbit height by two EPB (External Proton Beam) dipoles. The beam is then kept within the Main-Ring tunnel wall and made to follow the accelerator orbit closely, as seen in Fig. 3-4, by distributing horizontal bends evenly over positions F21 and F23 so that beam elements will not block the Main-Ring tunnel and impede normal maintenance activities. Finally, a counterclockwise bend near F25 brings the beam out through a penetration in the corner of an existing alcove at F25. Providing a tunnel penetration at any other point would require a long slot in the tunnel wall because of the small angles involved and the consequent weakening of the wall would be unacceptable.

The space around the F25 outward bend is very tight, and an EPB dipole cannot be placed in the alcove. This means the last bend, needing a total of five 10-ft EPB diples, encroaches upon tunnel space more than may be considered desirable. This can only be avoided by using special dipoles tailored to fit in the alcove, which must also house an Energy Doubler-Saver cold box down nearer the floor.

The extracted proton beam then enters a length of 10-in. pipe buried in the ground, which serves as a permanent radiation barrier for the next enclosure. In analogy with other Fermilab external-beam enclosures, we call the latter "$\bar{p}$ Hall". It contains the quadrupoles required to produce a highly focused beam spot on the production target in the next enclosure, the Target Vault. $\bar{p}$ Hall is accessible through a labyrinth, so that the elements there may be serviced *in situ* and the actual target may be reached by remote-handling devices. We note that it also contains four quadrupoles needed for the reverse-injection beam.

The Target Vault will be a high-radiation area, so that $\bar{p}$ Hall will be protected from residual activity and gas activation by a wall between it and the Target Vault. The 130-ft Target Vault immediately follows $\bar{p}$ Hall, with the target position as close as possible to the separating wall, as shown in Fig. 3-5. It will be possible to extract the target through the separating wall on a railway cart and store it in a lead pit in $\bar{p}$ Hall. The target itself is normally in a magnetic field, which bends the 80-GeV proton beam downward by 5 mrad. This ensures that radiation from the beam dump beyond the target will be directed into the ground and will not fill the following tunnel with radiation.

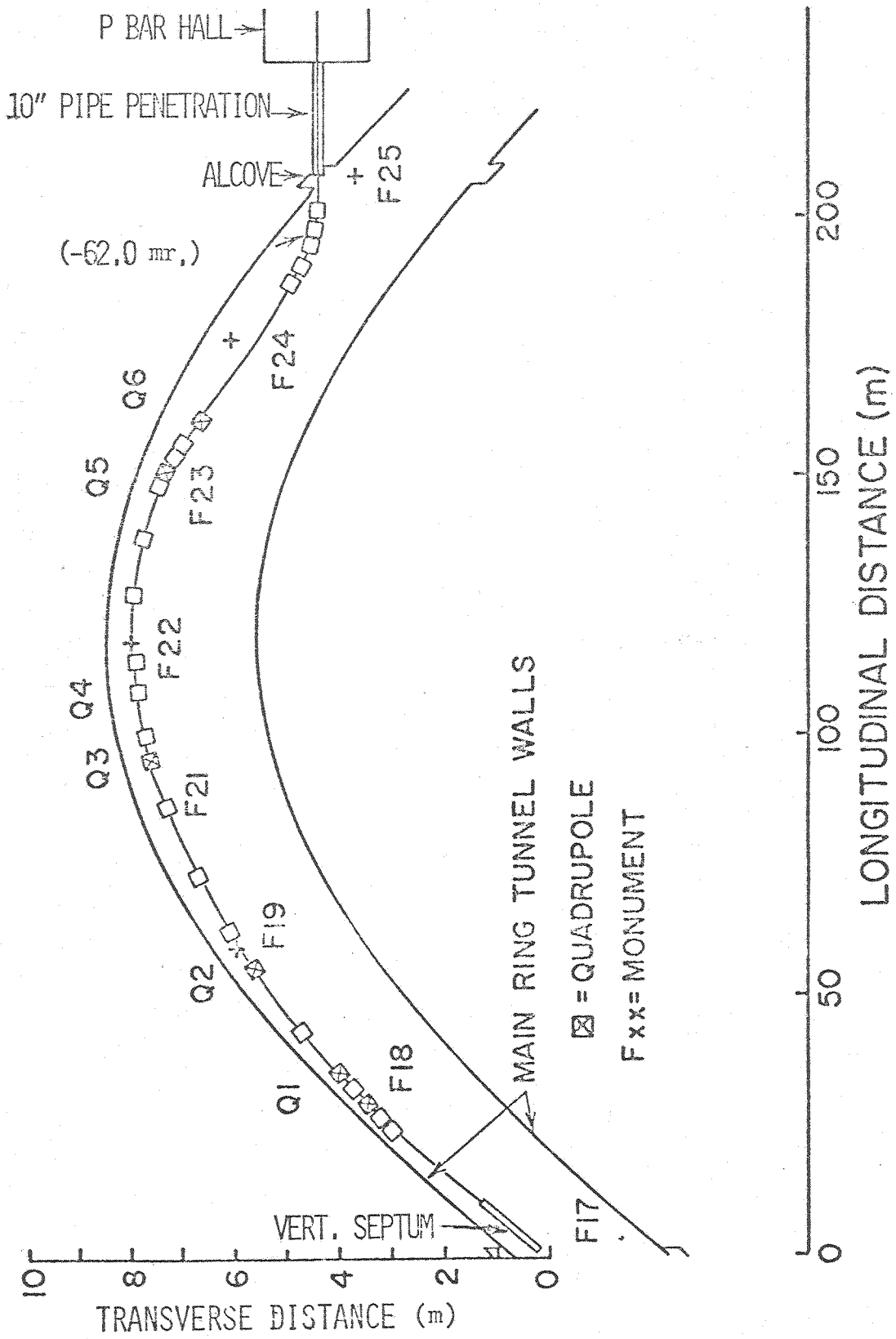

Fig. 3-4 Extracted-proton beam-transport layout.

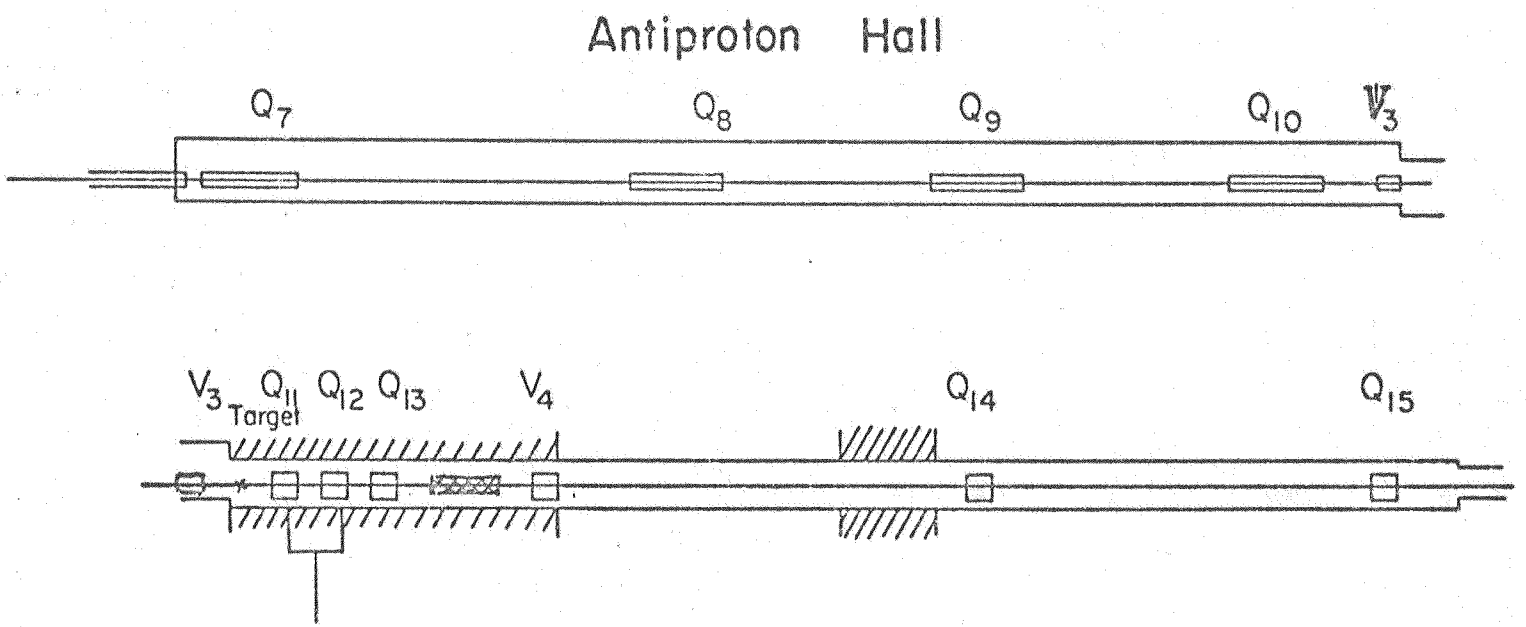

Fig. 3-5 $\bar{p}$ Hall and Target Vault

3.4 Spot Size and Divergence Angle

At any point along the length of the target, the antiprotons are produced from a spot the size of the proton beam at that point (if that size is smaller than the target size) with a divergence cone angle given roughly by the Cocconi angle (0.3 GeV/c)/p. For the systems considered here, the solid angle of acceptance of the antiproton cone is only about 2% of the total cone of antiprotons produced and the distribution of $\bar{p}$'s within the acceptance cone is therefore approximately uniform.

To maximize the number of $\bar{p}$'s collected from a given point along the target, the transverse dimensions of the incident p-beam at that point must be sufficiently small. This means that the depth of focus of the $\bar{p}$ collection system will also be small.

3.5 Antiproton Production Cross Section

Using existing experimental data, it is possible to estimate to ±50% accuracy[1] the $\bar{p}$ production cross section of 0° production of 4.5-GeV antiprotons with 80-GeV protons bombarding a heavy target.

Two conclusions that can be reached from this data are:

(i) The antiproton production cross section $d^2\sigma/dp\, d\Omega$ (at $X_F = 0$) for 80-GeV pp collisions is greater by a factor of 4 to 6 than for 26 GeV pp collisions.

(ii) The antiproton momentum for maximum yield from 80-GeV protons hitting heavy nuclei is between 3 and 6 GeV/c. The yield equation we use is[2]

$$\frac{d^2 N_{\bar{p}}}{dp\, d\Omega} = \frac{1}{\sigma_0} E \frac{d^3\sigma}{dp^3} p_{\bar{p}} x_{abs} I_p, \qquad (3\text{-}9)$$

where $\sigma_0 = 33$ mb is the pp inelastic cross section, $(E\, d^3\sigma/dp^3) = 0.8$ mb/Gev^2 is the estimated $pp \to \bar{p}$ invariant cross section for 80-GeV pp collisions, I_p is the number of protons hitting the target, and x_{abs} is the effective number of mean free paths of target. If the protons and antiprotons have an absorption m.f.p. of λ and L is the length of the target, then we have

$$x_{abs} = \frac{L}{\lambda} e^{-L/\lambda}. \qquad (3\text{-}10)$$

This never exceeds 0.4 and is 0.3 for a target whose actual length is $\lambda/2$.

3.6 Transverse Matching

The target efficiency is further decreased by the requirement discussed above that a very small proton-beam spot size is required to obtain a bright source of antiprotons. The real two-dimensional $\bar{p}$ yield into a fixed one-dimensional phase acceptance $\bar{\varepsilon}$ can be written

$$Y \propto \frac{d\bar{n}}{d\ell} \ell_{eff} \frac{\bar{\varepsilon}}{\bar{\beta}}, \tag{3-11}$$

where $\bar{\beta}$ is the envelope function of the antiprotons, ℓ_{eff} is the effective length of the target due to limited depth of focus of the $\bar{p}$ collection system, and $(d\bar{n}/d\ell)$ is the linear density of $\bar{p}$ production.

The effective length ℓ_{eff} (i.e. the equivalent depth of focus) is given by[1]

$$\ell_{eff} = 2 \int_0^{L/2} \frac{\beta_0 \bar{\beta}_0}{\beta \bar{\beta}} d\ell, \tag{3-12}$$

where β (or $\bar{\beta}$) is the betatron amplitude function for the protons (or antiprotons), and β_0, $\bar{\beta}_0$ are β, $\bar{\beta}$ evaluated at the focus at $\ell = 0$.

With no focusing field at the target, the integral in Eq. (3-12) can be evaluated to be $\ell_{eff} = 0.38$ L.

3.7 Focusing Within the Target

By passing a longitudinal current along the target rod, an azimuthal magnetic field that focuses antiprotons (and unfortunately defocuses protons) can be used as a field-immersion lens to increase the depth of field.[3] Described in another way, this field allows one to confine the antiprotons from the upstream part of the target so that they appear to be emitted by the downstream part of the target, thus increasing the brightness of the target. Since substantial engineering problems would be involved in pulsing large currents through a target wire, we have not included this feature in the present target design.

3.8 Target Design

To arrive at a practical target design, one must add to the foregoing factors such practical considerations as energy deposition in the target material. The emphasis on high-brightness production leads to peak instantaneous thermal energy density of the order of 15 kJ/cm^3. For this reason, we are giving serious consideration to a target of liquid mercury that will not explode during a beam spill and recover between spills.

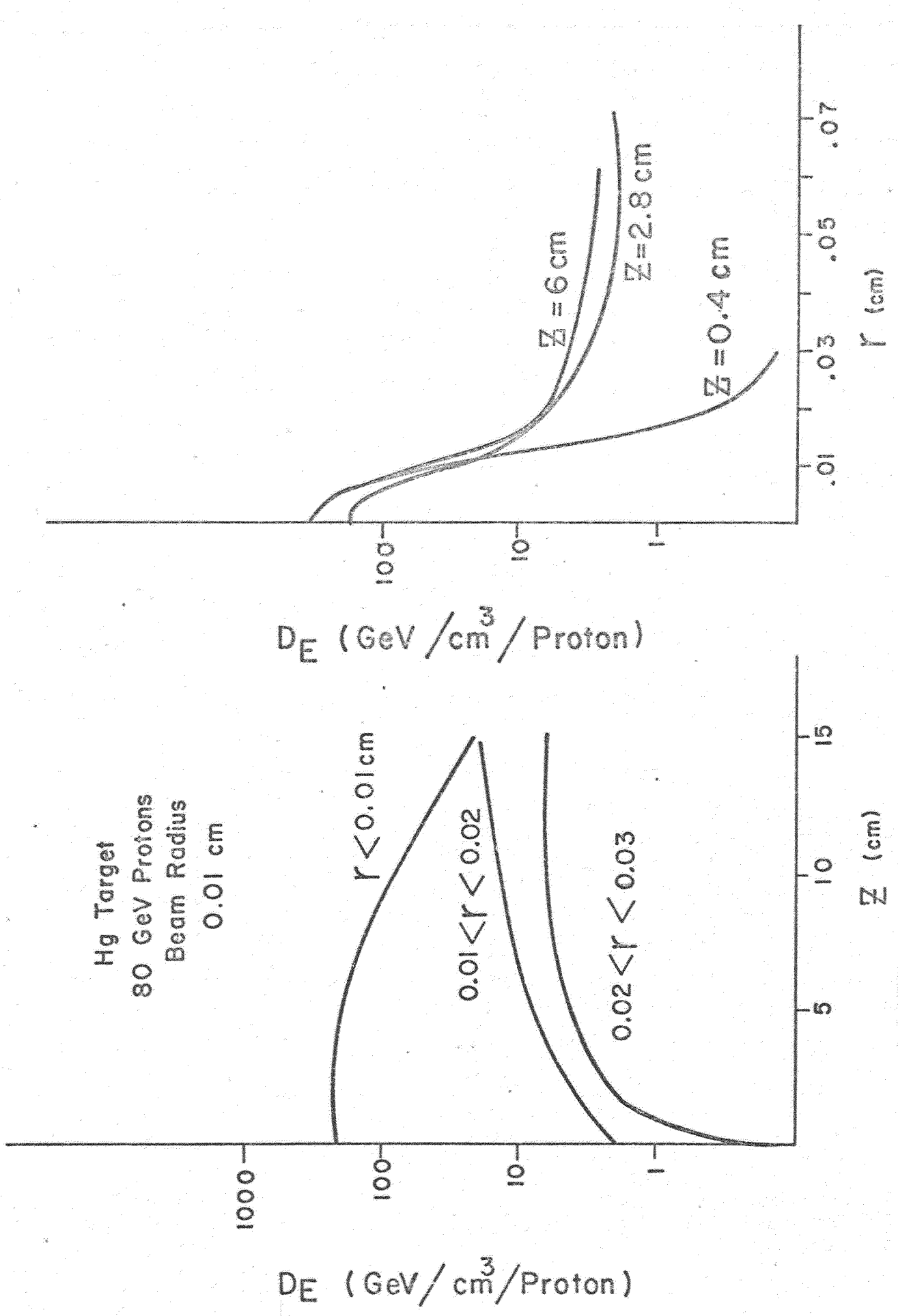

Fig. 3-6 Energy distribution in a mercury target.

Some additional design considerations are:

(i) The target assembly must fit the limited space that is available between the proton beam and the antiproton beam.

(ii) The target container must be large enough to reduce the pressure and temperature bump produced by the vaporization of the target material.

(iii) The container will have to handle:
  a. time-dependent loading;
  b. thermal shock;
  c. stress due to differential heating;
  d. creep stress due to constant pressure;

(iv) Liquid-metal embrittlement may occur unless a judicious choice is made of container material.

(v) Creep resistance becomes an increasingly important consideration at elevated temperatures, becoming the dominating design consideration for temperatures greater than half the melting temperature.

(vi) Wall thickness should be reduced to a minimum to lessen the tendency to fracture under shock.

(vii) The gas used around the vessel must be inert with the chosen vessel material.

(viii) Good heat conduction must be provided.

(ix) Radiological and chemical toxicity must be contained.

We have carried through a schematic design of target and container that aims towards optimization with respect to the above constraints. Compatibility between items (i) and (ii) has not been achieved in this design. The volume restriction for the target container, in conjunction with the permissible clearance between the primary and secondary beams, will require a change of the vessel cross section from circular to elliptical or a change in the beam transport. The choice among these alternatives can be made when other features of the targetry are more firmly established. The choice of optimum vessel thickness is established by a balance between rupture resistance on the one hand and fracture and differential heating on the other (items (iii c) and (vi)). The thickness chosen is appropriate for steel, which is a good choice for avoiding embrittlement caused by the mercury.

The energy deposition in the mercury target has been estimated using information from a detailed calculation. The magnitude of the thermal and mechanical transients has then been calculated. Figure 3-6 shows longitudinal and radial distributions

of energy density per incident proton for a beam of 0.1-mm radius. The energy deposited is 3.1 kJ per spill, of which 860 J goes into heat of vaporization and 2240 J goes into instantaneous (i.e. constant-volume) heating of the vapor. The pressure and temperature after expansion into the vessel volume are approximately 30 psi and 180°C. Even if these estimates are somewhat low, they suggest that there is no major problem in this respect. The critical consideration is the local instantaneous pressure and temperature at the beam windows.

Both the radiological and chemical toxicity of the target are matters of concern. The design incorporates reasonable shielding, redundant sealed containment, and maintenance-free installation. The only manipulation required for an activated target will be an infrequent total replacement. The target has no support requirements other than a closed-loop cooling system. The concerns of radiation-safety specialists have been included in the criteria that have resulted in the schematic design presented. A prototype target will be fabricated and tested in the coming months.

Table 3-II summarizes the target design parameters.

Table 3-II Target Design Parameters

Target Length, L		6 cm
β_0		1 cm
Spot radius $r_{\bar{p}}$		0.2 mm
Production angle		24 mrad
Target material		Hg
$\bar{p}$ energy		4.5 GeV
$\Delta p/p$	=	±2%
Solid angle (eff)	=	10^{-3} ster*
Absorption length	=	12 cm
Eff. no. of abs. lengths	=	0.30
$F_{geom} = \ell_{eff}/L$	=	0.38

*In principle this number could be as large as 1.8×10^{-3} ster for the indicated production parameters. The smaller value was chosen to reflect the fact that the vertical admittance of the Electron Cooling Ring is about half the horizontal.

Then we can estimate the yield as

$$N_{\bar{p}}/N_p = \frac{1}{\sigma_0} E \frac{d^3\sigma}{dp^3} p_{\bar{p}} \Delta_{\bar{p}} \Delta\Omega \, x_{abs} F_{geom}$$

$$= \left(\frac{1}{33}\right) (0.8) (5.4) (0.22) (10^{-3}) (0.30) (0.38)$$

$$= 3.2 \times 10^{-6}$$

This value for $N\bar{p}/Np$ is consistent with that calculated by Chadwick[4] using a rather different procedure. It is smaller than the (scaled) yield obtained by Pondrom[5] apparently mainly because F_{geom} was taken to be unity in Pondrom's calculation.

3.9 Beam Transport from $\bar{p}$ target to Precooler

This transport line carries a beam of 4.5-GeV antiprotons to the Precooler. The solid-angle acceptance of the system is defined by the $\bar{p}$-collection quadrupole triplet at approximately- $\pi \times (24 \times 10^{-3})^2$ or 1.8×10^{-3} sr (semicone acceptance angle of 24 mrad). Since the admittance of the Precooler is 4.8×10^{-6} m-rad in each plane at 4.5 GeV, the primary-beam focus should be less than 0.37 mm in radius. An achromatic match to the Precooler is required for the $\Delta p/p = \pm 2\%$ $\bar{p}$ beam, and therefore a substantial portion of the transport must consist of a chromatic-correction section.

The design is subject to the following physical constraints:

(i) the $\bar{p}$ beam rises in elevation by 0.1874 m from the target to the center of dipole V4;

(ii) The distance from $\bar{p}$ target to Precooler must be less than 175 m;

(iii) the Precooler is sited 10 ft (3.048 m) in elevation above the $\bar{p}$ target.

The vertical translation of the system is sketched in Fig. 3-7. A vertical dipole (V5) is powered to kick the 4.5-GeV $\bar{p}$ beam up by 2.8125°. It rises to Precooler elevation and is brought flat and made achromatic by the dipole V6. This rise occupies 191 ft (58.2 m) and is a conventional translation system. Quadrupole focusing is of course required to maintain reasonable beam size. V6 is followed by transport in the horizontal plane to the injection point into the Precooler; the elements of this beam transport are shown in Fig. 3-8.

It is planned to inject the $\bar{p}$ beam into a dispersion-free straight section of the Precooler where the beam characteristics are $\beta_x = 16.48$ m, $\beta_y = 26.52$ m, and $\alpha_x = 1.19$ and $\alpha_y = 0.34$. Furthermore the beams should be achromatic. That is, the phase-space ellipses for all $\Delta p/p$ should be nearly identical. Thus it will be necessary to correct for the quadrupole chromatic aberrations by using sextupole magnets suitably placed in a periodic channel, such as suggested by Brown.[6] We assume the same periodic structure as used in the Precooler design, i.e., a cell length of 9.119 m and a phase shift of 90° per period. The correction section is chosen to be made up of 8 cells with total phase shift of 4π. Bending magnets are placed midway between F and D quadrupoles, with one missing at the midpoint, so that 16 dipoles are required. The system will first bend to the left in the first 4 cells and then bend back an equal amount in the final

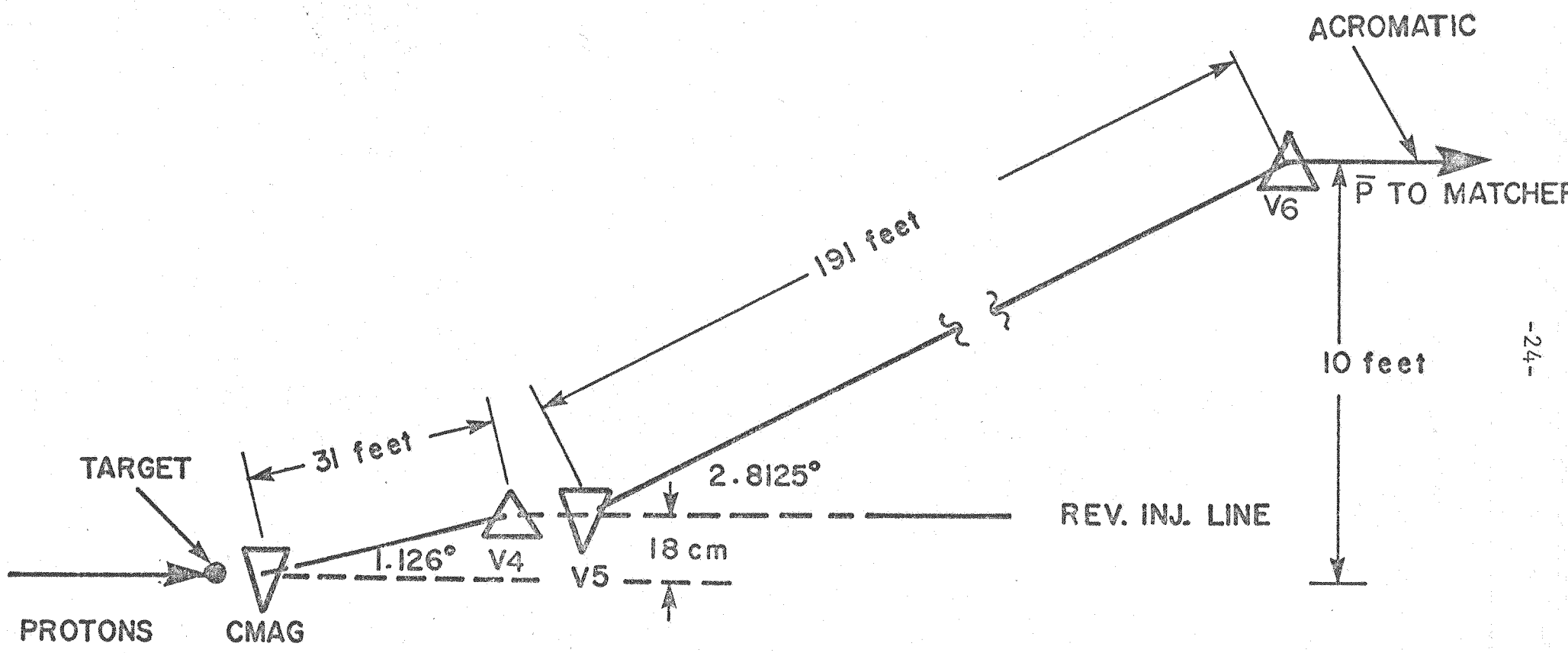

ELEVATION VIEV

Antiproton Vertical Translation Systems

Fig. 3-7 Vertical translation of the $\bar{p}$ beam.

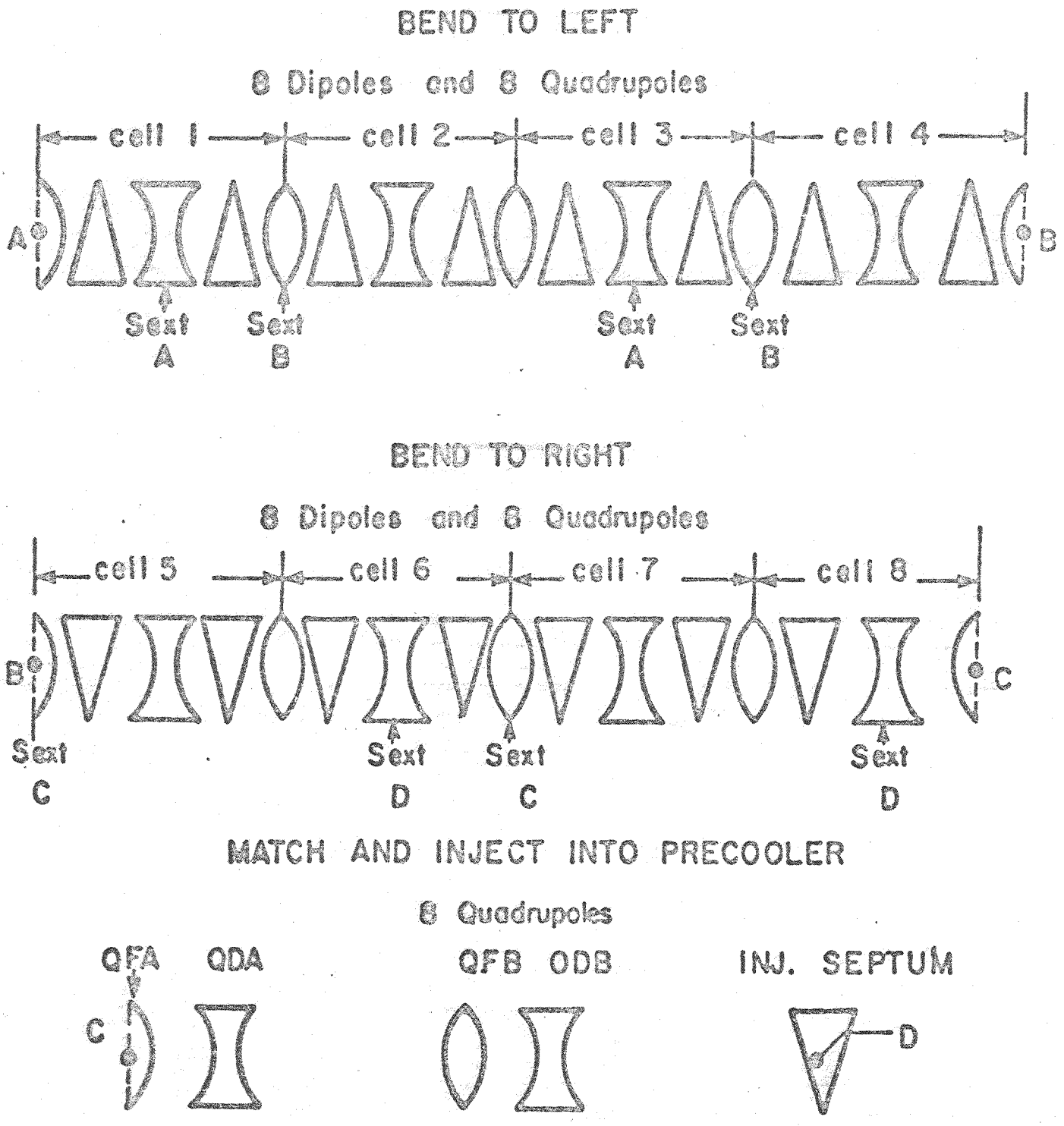

Fig. 3-8 Optics of the $\bar{p}$ beam.

four cells, such as is shown in Fig. 3-8. We do not specify the bends precisely at this time, but it is reasonable to assume a bend of 40° per 2π section or 5.0° per magnet.

It is necessary to construct a matching section from V6 to the point A of the chromatic corrector. At point A the lattice parameters are β_x = 15.231 m, β_y = 2.7255 m, $\alpha_x = \alpha_y = 0$ and the beam is achromatic. Point B represents the transition between the two 120-ft correctors. At point C, the beam enters the final matching section (at QFA) and is transported to the injection septum at point D in Fig. 3-8. This matching section is identical to that in the lattice, except that the dipoles are missing.

We believe that four sextupole families are required to achieve the achromatic beam conditions at point D. The two identical members of a family are spaced by π phase shift to cancel the geometric aberrations. A possible configuration for locating the sextupole families is also indicated in Fig. 3-8. The sextupole windings are included in the quadrupoles.

This design is discussed in more detail in Ref. 7.

References

[1] J. W. Cronin, 1977 Fermilab Summer Study, Vol. 1, p. 269.

[2] D. Cline, P. McIntyre, F. Mills and C. Rubbia, Collecting Antiprotons in the Fermilab Booster and Very High Energy $\bar{p}p$ Collisions, Fermilab Internal Report TM-689, 1976.

[3] D. Cline and F. Mills, Exploding Wire Lens For Increased-$\bar{p}$ Yield, Fermilab $\bar{p}$ Note 7, Jan. 1979.
L. C. Teng, Study of Current-Carrying $\bar{p}$ Production Target, Fermilab $\bar{p}$ Note, Feb. 1979.

[4] G. Chadwick, Considerations on the Antiproton Production Beam, Fermilab Note, Aug. 1977.

[5] L. G. Pondrom, 1977 Fermilab Summer Study, Vol. 1, p. 259.

[6] K. L. Brown, private communication.

[7] E. Colton, Optics Design From $\bar{p}$ Target to Precooler, Fermilab $\bar{p}$ Note 46, Oct. 1979.

4. STOCHASTIC COOLING AND DECELERATION IN THE PRECOOLER

4.1 Introduction

An unbunched pulse of antiprotons is to be injected into the Precooler with a kinetic energy of 4.5 GeV, a momentum spread of ±2%, and betatron emittance of $4.8\pi \times 10^{-6}$ mrad in each plane. For the Booster-circumference Precooler ring envisioned, this corresponds to a longitudinal phase-space area of 340 eV-sec. Because of the limitations imposed by the electron-cooling process, the Electron Cooling Ring requires something between 1 and 3 eV-sec. This section describes the stochastic cooling and rf decelerating processes utilized in the Precooler to effect the necessary phase-space area and energy reductions.

4.2 Stochastic Cooling Theory

Following the invention by van der Meer[1], the theory of stochastic cooling has been developed in various levels of detail, and with different approaches in a number of papers.[2-4] At present, one feature of the technique is that momentum cooling using notch-filter methods appears to be much faster than transverse cooling. The antiproton collection scheme presented in this report recognizes this fact and incorporates only momentum cooling. Should techniques eventually be developed to speed up transverse stochastic cooling appreciably, the collection scheme could advantageously add it, but is not now part of the system.

Our knowledge of stochastic momentum cooling has greatly improved during the last year through analytical and computer investigations[5-8] to the point where we believe we have a workable cooling-system design. Our calculations predict adequate performance and appear to be consistent with calculations and experiments conducted by CERN.

In the notch-filter method used, information regarding a particle's momentum is obtained though its relationship with its revolution frequency. A filter system in the pickup-kicker chain appropriately conditions signals to accelerate or decelerate particles toward a specific rotation frequency (i.e., momentum). A useful filter element for this purpose is a shorted transmission line whose length corresponds to half the rotation period. Such an element exhibits "zeroes" in its input impedance at all harmonics of the rotation frequency. The resultant transfer function of such an element, when used in a voltage-divider configuration, appears as a series of notches, hence the term "notch filter".

Figure 4-1 shows the results of a typical computer simulation. The choice of the dispersion $\eta = 0.02$ is particularly significant. It provides for operation of the Precooler between 200 MeV and 8 GeV without crossing transition γ, and provides proper phase mixing, as will be described in the following sections.

Fokker-Planck Simulation of Δp/p Cooling

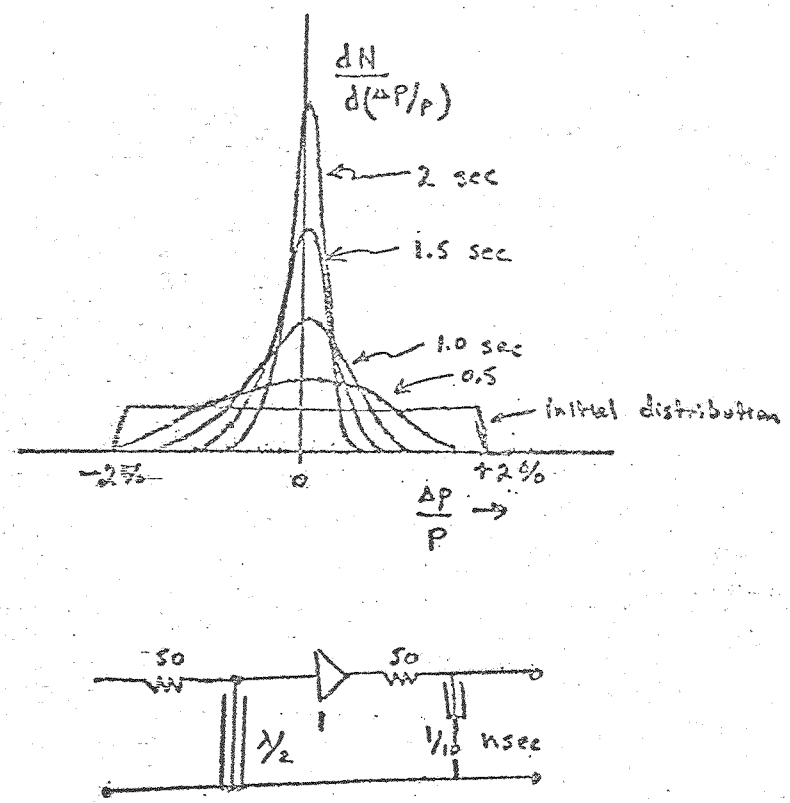

Booster-sized Precooler
Energy = 4.5 GeV
No. of $\bar{p}$ = 5 × 10^7
Initial p spread = ±2%
η = 0.02
BW = 500 MHz (200-700 MHz)
No. of P.U. = 200
Times shown: 0, 0.5, 1.0, 1.5, 1.0 sec.
Gain = 1.5 × 10^9 ; Preamp Noise Figure: 2db
1/4 turn separation between pickups and kickers

Fig. 4-1 Computer simulation of notch-filter momentum cooling.

4.3 Cooling Sequence

4.3.1 Choice of Optimum Cooling Steps. The essential ingredient in stochastic momentum cooling with the notch-filter technique is the revolution-frequency spread. A requirement for optimal cooling is that the notch at the highest harmonic in the feedback-system bandpass be filled with beam signals. As cooling proceeds, the frequency spread decreases and the notch gaps are less and less filled, until a situation is reached where the cooling is grealy reduced. By decelerating a cooled beam, the required frequency spread can be restored to make rapid cooling possible again.

The criterion that the width of the highest Schottky band at frequency $h\omega$ equal the notch width may be written as

$$h\Delta\omega = \text{const.} \tag{4.1}$$

But

$$\frac{\Delta\omega}{\omega} = \eta \frac{\Delta p}{p} \tag{4.2}$$

and it follows that

$$\frac{\eta}{\beta} \frac{\Delta p}{p} = \text{const.} \tag{4.3}$$

Eq. (4.3) can then be used to calculate the energy required to restore the initial mixing.

The cooling scheme we have developed will reduce the momentum spread by a factor 5 in 2 seconds or less at 4.5 GeV. After the beam has been cooled, it will be bunched at some harmonic number h and decelerated. One can stop the deceleration at 2.6 GeV and re-apply stochastic cooling with the same technique (but a slightly altered filter) to achieve a further reduction of $\Delta p/p$ by a factor 5 in 2 seconds. Obviously the deceleration ramp should first be flattened and the beam adiabatically debunched to avoid too-large dilution. After cooling, the beam will again be adiabatically rebunched and further decelerated.

The frequency-spread condition of Eq. (4.3) for stochastic cooling will again be met at a kinetic energy of 1.3 GeV. The beam will again be adiabatically debunched at constant field, cooled once more in 2 seconds with one more reduction of $\Delta p/p$ by a factor 5, adiabatically rebunched and decelerated finally to 200 MeV. Figure 4-2 is a schematic representation of the cooling process. Table 4-I gives the $\bar{p}$-beam momentum spread at the end of each cooling and decelerating step, together with other parameters, such as the total beam phase-space area S. The momentum spreads are for fully adiabatically debunched beams. No

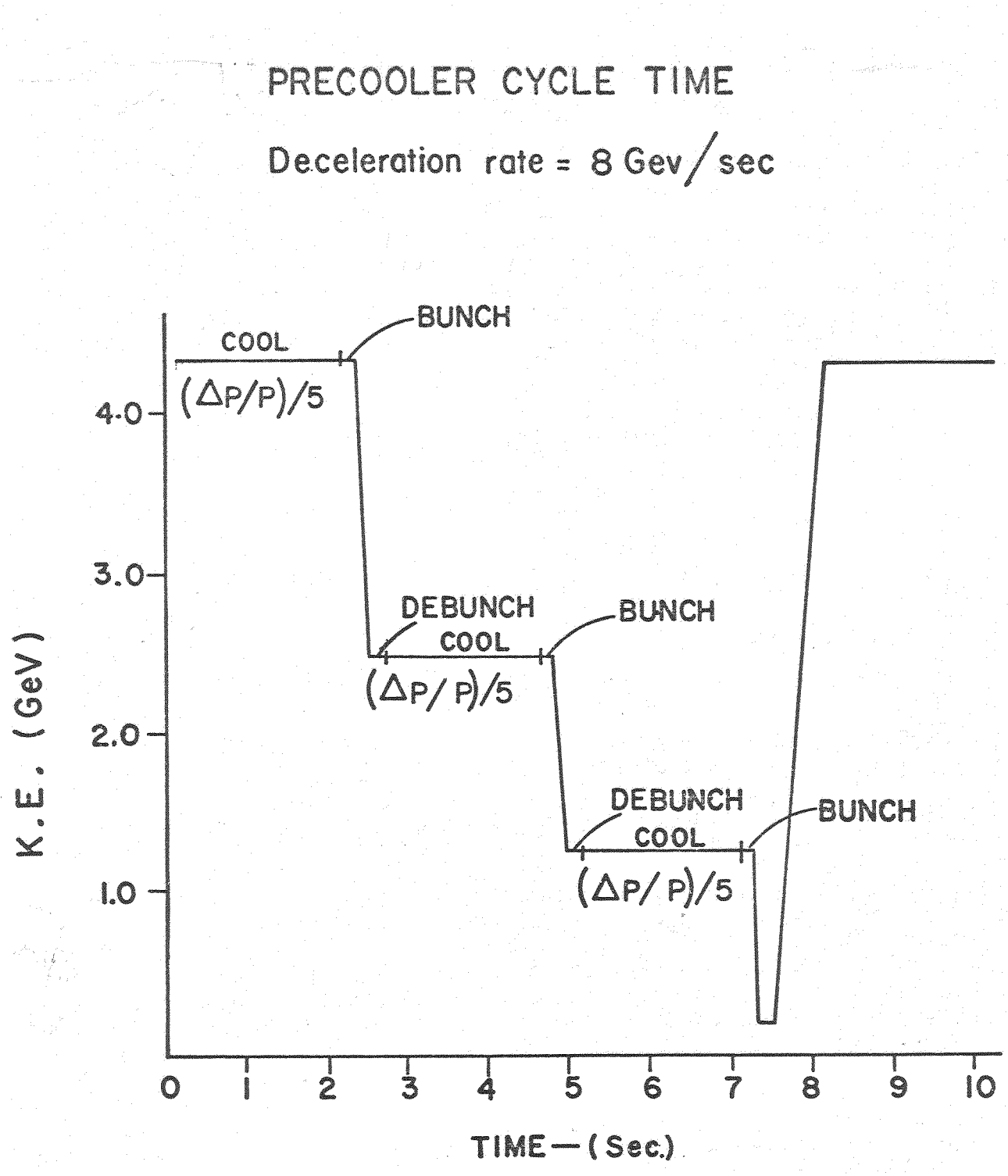

Fig. 4-2. Schematic plan of the cooling process.

Table 4-I Parameters for Stepped Stochastic Cooling

Kinetic Energy T(GeV)	Momentum p(GeV/c)	Momentum Spread $\Delta p/p$(±%)	Phase- Space Area S(eV-sec)	
4.5	5.36	2.0	340	
	after stoch cool (1)	0.4	68	
2.6	3.41	0.63	68	3
	after stoch cool (2)	0.13	14	steps
1.3	2.03	0.21	14	
	after stoch cool (3)	0.042	2.7	
0.2	0.644	0.133	2.7	
or				
0.53	1.13	0.075	2.7	optional
	after stoch cool (4)	0.015	0.54	4th step
0.2	0.644	0.027	0.54	

dilution has been included for deceleration and the debunching-rebunching processes. As shown in the Table, the final momentum spread (debunched) at 200 MeV is ±0.133% after three cooling steps. It is possible to perform a fourth period of cooling at 530 MeV; in this case $\Delta p/p$ = ±0.0266% at 200 MeV. We might well find that stochastic cooling is more effective than we believe and that three steps of cooling will be adequate to achieve a momentum spread that can be accommodated in the present Electron Cooling Ring. Otherwise we can utilize four steps of cooling. The scheme we have outline for the Precooler is flexible enough to allow such variation in tactics.

4.3.2 Hardware Requirements. The same pickup, amplifier, and kicker system can be used for all cooling steps, although either separate notch filters (high-quality long transmission lines) or a tunable system are required because of the variation of β, and consequently of the revolution frequency, during deceleration. Because of this same variation of β, the delay between pickups and kickers must also be adjusted. Relatively fast switches can connect the preamplifier stages to the several notch filters and delay lines.

4.3.3 Requirement of Deceleration It is not desirable to accelerate at a high rate in the Precooler because a high rate would increase the rf system requirements with minimal gain in the cycle time. Thus a metallic vacuum chamber can be used without appreciable chamber heating or induced sextupole fields from the eddy currents.

The most stringent requirements for the rf deceleration system will be encountered during the first step of deceleration from 4.5 GeV down to 2.6 GeV. In this step, the beam has the largest energy and phase-space area. If the deceleration occurs in a period of 0.2 sec, the energy loss per turn is

$$\Delta E = eV \sin\psi_s = 8.0 \text{ keV/turn.}$$

The rf voltage required to supply a bucket with an area at least equal to the beam bunch area (68/h eV-sec) is

$$\frac{V}{h} = 65 \text{ kV.}$$

The smallest rf bucket area occurs at 2.6 GeV and is approximately equal to the bunch area. The voltage requirement through the deceleration cycle is shown in Table 4-II. V_{ad} is the voltage required to create stationary buckets with the same bunch area. V_{max} is the maximum voltage required for bucket area at the end of each deceleration step. The number in parentheses is the ratio of the bucket area to the bunch area corresponding to V_{max} and to decelerating at a constant rate of 8 keV/turn.

Table 4-II Voltage Requirement Normalized to Harmonic Number h

Kinetic Energy GeV	S V-sec	V_{ad}/h kV	V_{max}/h kV	
4.5	68	6.5		
2.6		34	65	(1)
2.6	14	1.35		
1.3		6.6	26	(2)
1.3	2.7	0.3		
0.2		1.7	26	(3)
1.3	2.7	0.3		
0.53		1.3	26	(2.4)
0.53	0.54	0.053		
0.2		0.068	10	(1.2)

We observe that the harmonic number is still a free parameter that one may choose in the most convenient way. One choice would be h = 1. There are therefore the following requirements for the rf system: it should provide a total of 65 kV and operate in the frequency range from 357.93 kHz to 622.72 kHz. The system can be accommodated in one of the four 20-m long dispersion-free straight sections.

4.3.4 Adiabatic Capture and Debunching. The beam should be adiabatically debunched before a cooling step and adiabatically recaptured at the end to avoid excessive phase-space area dilution. The rule we follow here is to turn the rf voltage on or off slowly according to a prescribed curve in a time that is

approximately one phase-oscillation period at the voltage V_{ad} given in Table 4-II. The phase-oscillation period is approximately constant at a value of 25 msec. This time therefore gives negligible contribution to the total cycle time of the Precooler. The total cycle time is then as follows:

(3 or 4) × 2 sec (for stochastic cooling)

+

1 sec for deceleration

+

1 sec to ramp to original field

=

8-10 seconds.

In conclusion, every 8-10 seconds a beam of 6×10^7 $\bar{p}$ with a transverse emittance of $4.8\,\pi \times 10^{-6}$ m-rad in each plane and longitudinal emittance of 0.55 eV-sec at 200 MeV is transferred to the Electron Cooling Ring.

There is an apparent bottleneck at 200 MeV, at the end of the Precooler cycle. When the 200-MeV beam is bunched to Electron Cooling Ring length, the momentum spread in the given bucket area becomes too large for the Electron Cooling Ring to cool in a reasonable time. This bottleneck can be avoided in any of several possible ways:

(i) Rebunch on the 2nd harmonic in the Precooler and inject and cool the two bunches sequentially. This could lengthen the total cycle time to 10 seconds.

(ii) Do the fourth cooling step. This will reduce the momentum spread, but will lengthen the total cycle to 10 seconds.

(iii) Achieve more cooling per step.

There are uncertainties in the estimates of stochastic cooling and of dilution in the rebunching process and it may well be that the three-step cooling and first-harmonic bunching will produce an acceptable momentum spread. With this uncertainty in mind, we are designing the rf system with enough frequency capability to cover (i).

It may be possible to avoid debunching and recapture of the beam by applying stochastic cooling to a long bunch trapped by a stationary rf bucket. Since the required cooling time is much larger than a phase-oscillation period, there is some incompatibility between cooling and mixing when they are

influenced by phase oscillations. The cooling of bunched beams needs further analysis and evaluation before it is included in the design.

Figure 4-3 is a conceptual layout of the momentum-cooling system for the Precooler.

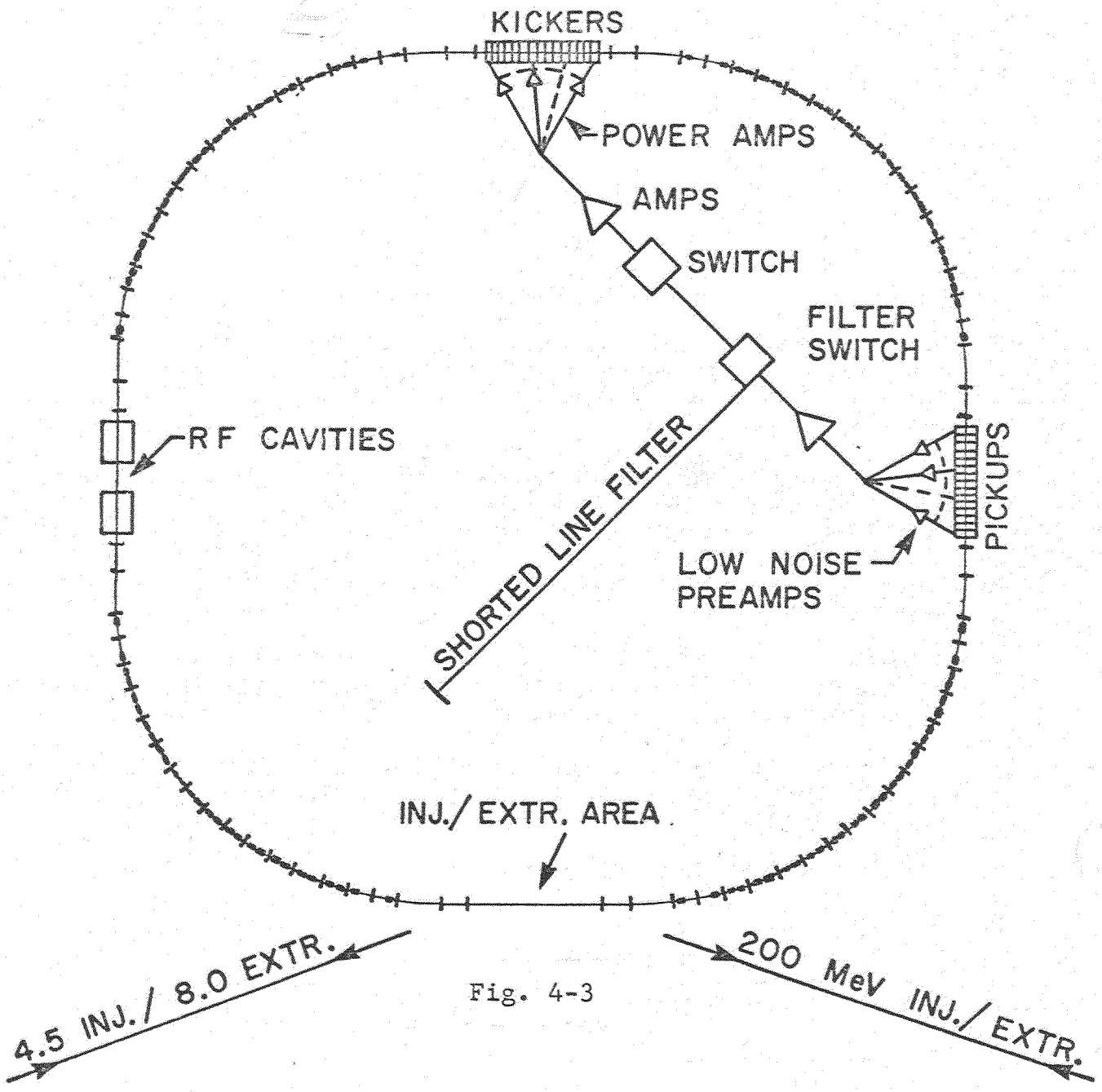

Fig. 4-3

CONCEPTUAL LAYOUT OF PRECOOLING SYSTEM

References

[1] S.van der Meer, Stochastic Cooling of Betatron Oscillations in the ISR. CERN-ISR-PO/72/31 (1972).

[2] F. Sacher, Stochastic Cooling Theory, CERN Report IST/TH 78-11 (1978).

[3] G. Carron and L. Thorndahl, Stochastic Cooling of Momentum Spread by Filter Techniques, CERN Report 2RF/78-12 (1978).

[4] D. Mohl, Stochastic Cooling, CERN Report PS/D7/78-75 (1978).

[5] A. Ruggiero, Computer Simulation of Momentum Stochastic Cooling, Fermilab $\bar{p}$ Note 10, Jan. 1979.

[6] A. Ruggiero, Program ST COO to Simulate Stochastic Cooling, Fermilab $\bar{p}$ Note 15, Jan 1979.

[7] E. Crosbie, Fermilab $\bar{p}$ Note 13, July 1979.

[8] J. Simpson, Deceleration in the Precooler, Fermilab $\bar{p}$ Note 20, Aug. 1979.

5. PRECOOLER RING DESIGN

5.1 Design Considerations

The requirements placed on the Precooler design by the antiproton collection scheme can be summarized as follows:

(i)	average radius	75 m
(ii)	momentum dispersion function (at 4.5 GeV)	0.02
(iii)	momentum acceptance	±2%
(iv)	transverse acceptance (with $\Delta p/p = \pm 0.13\%$)	$40\ \pi \times 10^{-6}$ m-rad
(v)	dispersion-free straight section length	> 20 m
(vi)	peak operating energy	8.0 GeV
(vii)	transition energy	>8 GeV
(viii)	highest practical superperiodicity	
(ix)	acceleration and deceleration rate up to	8 GeV/sec
(x)	deceleration from 4.5 GeV to 200 MeV	
(xi)	acceleration from 200 MeV to 8 GeV	

A study was made of the feasibility of using the recently decommissioned Argonne ZGS magnet ring as a basis for a Precooler and the results were presented in draft form in a study report in July, 1979. There were a number of drawbacks in use of the ZGS magnets, notably a necessarily low γ_t, low periodicity, large and expensive hardware (vacuum system, quadrupoles, etc), and a large containment structure and shield. A more suitable design, using new magnets, has been developed; it will meet all the requirements at a cost no more than that associated with the use of the ZGS magnets.

5.2 Lattice

These specifications have been met in a strong-focusing FODO design with 4 matched long straight sections and missing-magnet dispersion matching. A layout of the Precooler ring is shown in Fig. 5-1 and parameters are collected in Table 5-I. The lattice sequence and orbit functions are shown in Fig. 5-2.

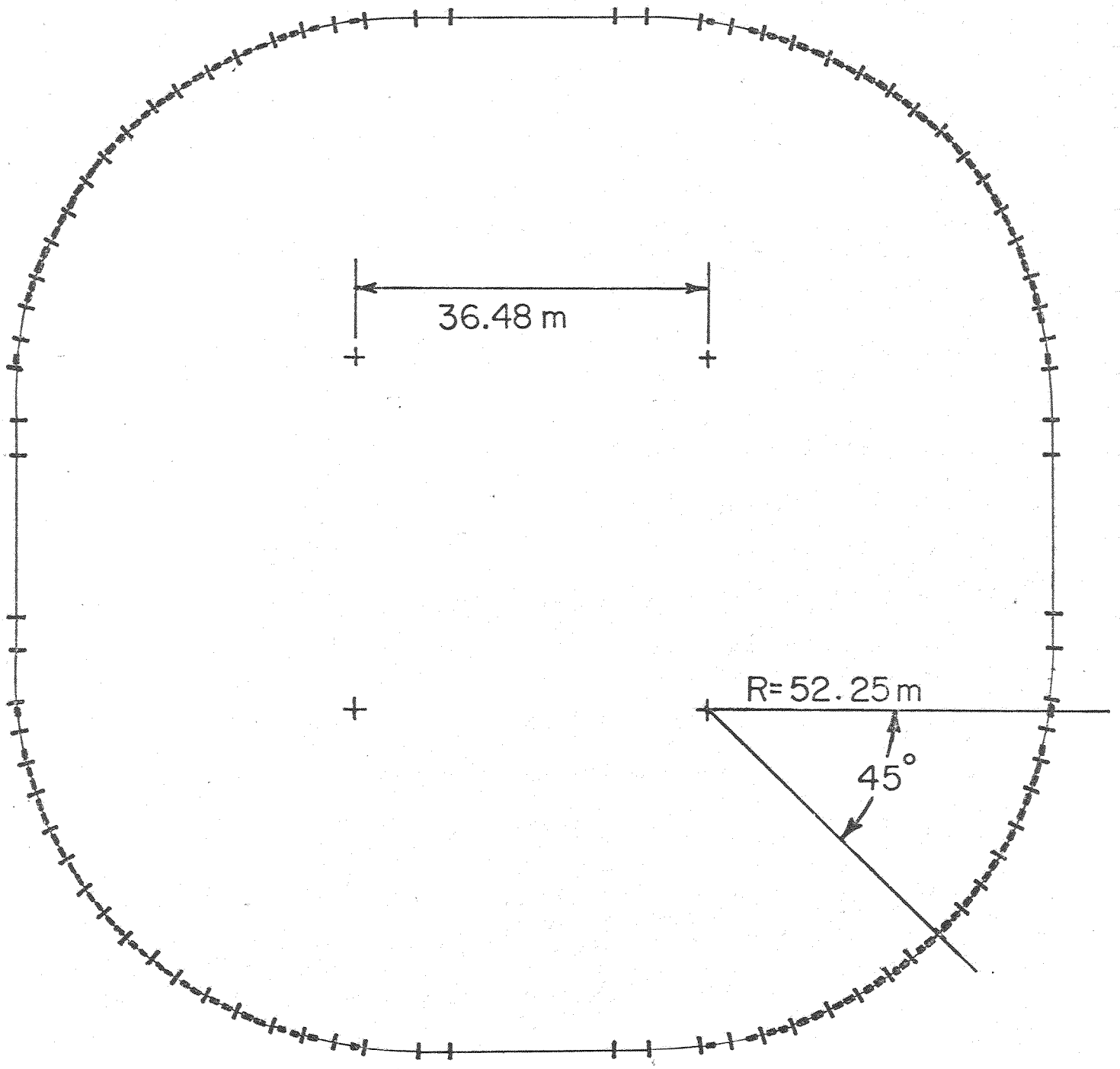

Precooler Layout

Fig. 5-1

- Dipole magnet

I Quadrupole magnet

20m / inch

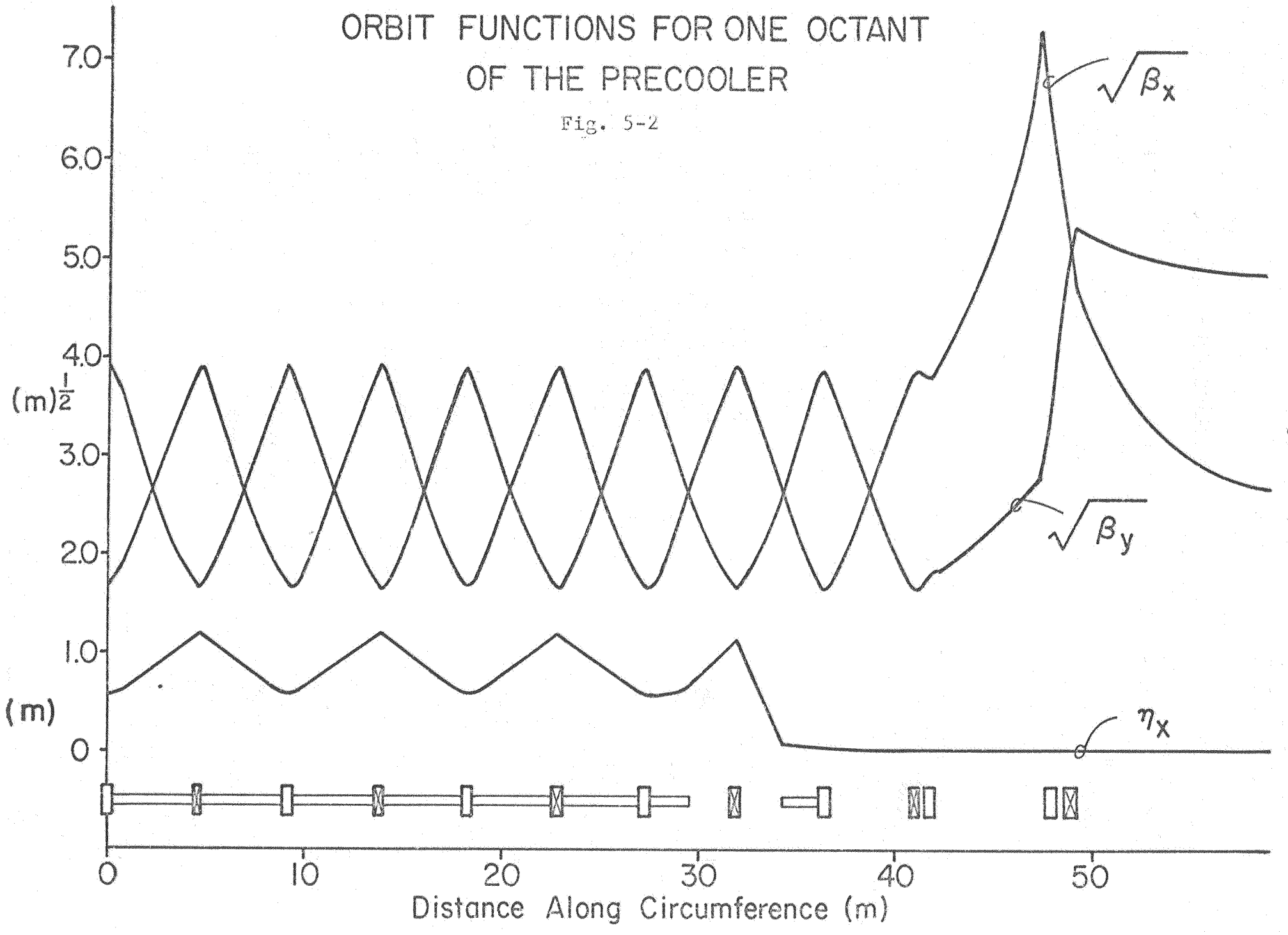
ORBIT FUNCTIONS FOR ONE OCTANT
OF THE PRECOOLER
Fig. 5-2
7.0
6.0
5.0
4.0
3.0
2.0
1.0
0
(m)^1/2
(m)
$\sqrt{\beta_x}$
$\sqrt{\beta_y}$
η_x
0
10
20
30
40
50
Distance Along Circumference (m)

Table 5-I Precooler Parameters

Superperiodicity		4
Long drift sections, disperion free		
length		20.2 m
number		4
Drift sections, disperion matching		
length		2.3 m
number		16
Average radius		75.47 m
Betatron tunes		
ν_x		10.7
ν_y		11.7
Phase advance per normal cell		90°
Transition γ		9.63
Revolution period (at 4.5 GeV)		1.6 μs
Dispersion $\eta = (\Delta t/t)/(\Delta p/p)$ @ 4.5 GeV		0.02
Orbit functions, maximum values		
$\hat{\beta}_x$		53.5 m
$\hat{\beta}_y$		28.1 m
$\hat{x}_p$		1.1 m
Lattice structure		
Half cells	DF:	QD O B OO B O QF
	FD:	QF O B OO B O QD
Normal cell	C:	DF FD
Dispersion matching all	CXP:	QD O1 B 02 QF 02 B 01 QD
Half straight sections	SS:	QFA 00 QDA QDA 03 QFB 04 QDB LL
Octant	OCT:	C C C CXP DF SS
Ring	RING:	4 (OCT $\overline{\text{OCT}}$)
Lattice components		
bending magnet B		
field at 8 GeV		9.35 kG
length		1.52 m
gap height		6.0 cm
gap width between coils		16.0 cm
copper weight (raw material)		200 kG
iron weight (raw material)		1500 kG
number used		128
normal quadrupoles 2QF, 2QD, 2QDA		
gradient at 8 GeV		≤160 kG/m
length		.61 m
pole-tip radius		4.8 cm
pole-tip field		≤7.8 kG
copper weight (raw material)		100 kG
iron weight (raw material)		1100 kG
number used		80
special matching quads QFB, QDB		
gradient		≤137 kG/m
length		.91 m
pole-tip radius		7.0 cm
pole-tip field		≤9.6 kG
number used		16

The horizontal magnet aperture is determined by the momentum spread at 4.5 GeV; the vertical aperture is set by the transverse emittance at 200 MeV. The majority of the quads are 2 ft long with a 4.8-cm pole-tip radius. In the matched straight sections, a large-aperture doublet is needed at both ends of the long drift space. These quads are 4 ft long and have a 7-cm pole-tip radius.

5.3 Injection and Extraction

It must be possible to inject at 4.5 GeV, to extract at 200 MeV, inject again at 200 MeV and finally to extract at 8.0 GeV. The necessary injection and extraction hardware consists of a low-energy set and a high-energy set. Each set can serve both functions because the directions of the beam circulation in the Precooler are opposite for the deceleration and acceleration processes. Both high-energy and low-energy systems are located in a single dispersion-free drift space. Both systems are horizontal full-aperture kickers and magnetic septa separated by 90° of betatron phase. The 200-MeV kicker is near one end of the drift space and the septum is close to the other end. The high-energy system has its kicker near the 200 MeV septum. Both systems require rise and fall times of approximately 200 nsec for 90% filling of the ring. The bunch-by-bunch extraction of the 8-GeV beam discussed in Sec. 5.7.2 requires a rise time of approximately 70 nsec. For a horizontal emittance of 10^{-6} m-rad at 8 GeV, a 1.5-m, 200-G kicker will provide the displacement needed to clear a 1-cm magnetic septum. There is adequate space for all these components in the drift space.

We will not discuss the 200-MeV transport between the Precooler and Electron Cooling Ring in any detail. It is a simple, straightforward system.

5.4 Magnet Design

The magnet system designed and constructed for the Fermilab Electron Cooling Experiment Ring has successfully achieved the designed field values and stringent tolerances. Figures 5-3 and 5-4 indicate the measured dipole and quadrupole fields as evidence of their quality.

Although these particular magnets are not suitable for the Precooler, they are an indication of the capability of the design, which has been adapted for the Precooler magnets. The peak dipole field required (8 GeV in the Precooler) is 9.4 kG. A dipole magnet design capable of meeting this and the aperture requirements is shown in cross section in Fig. 5-5. A corresponding quadrupole design is shown in Fig. 5-6. Parameters of the magnets are given in Table 5-I.

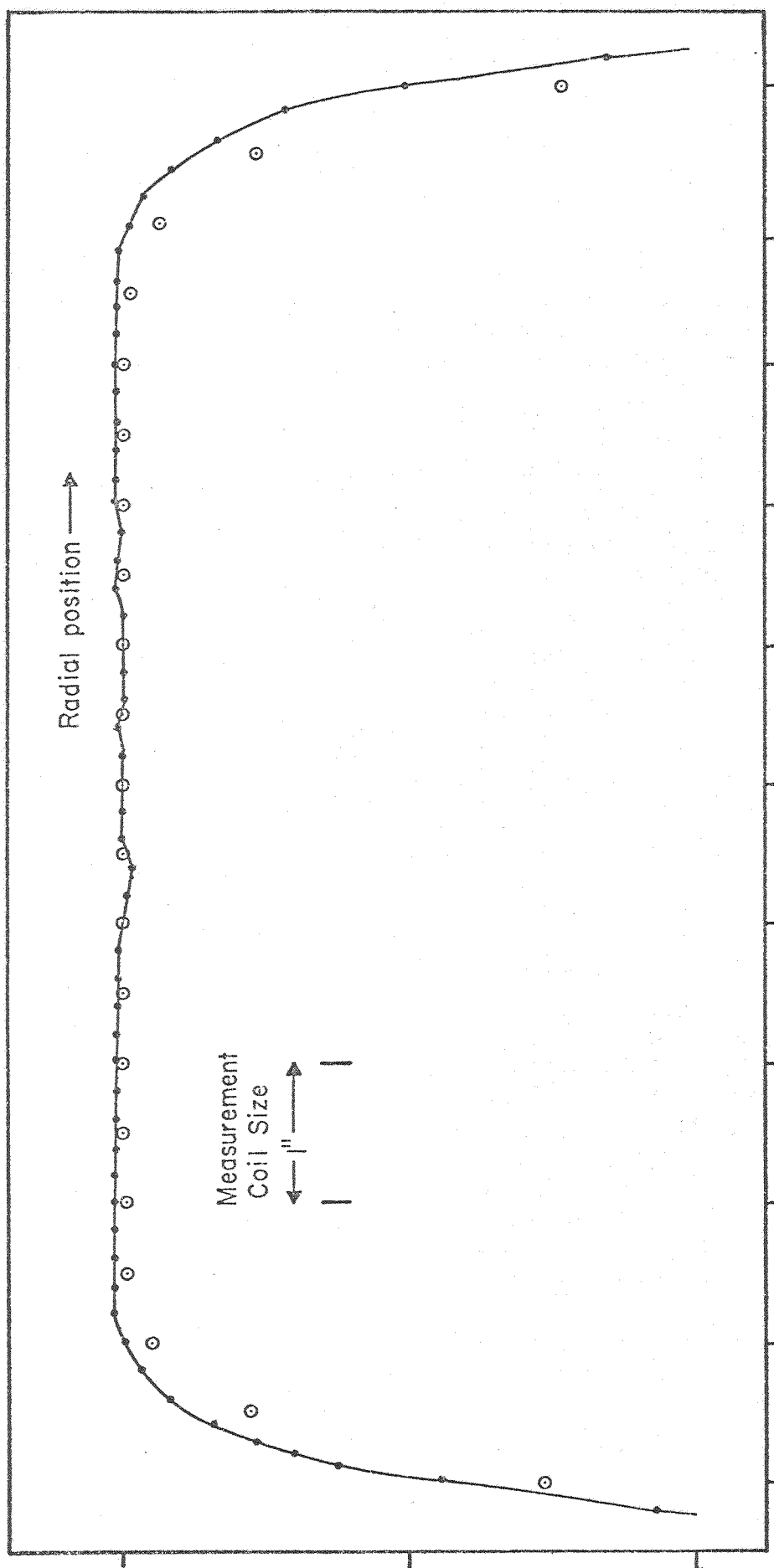

Fig. 5-3 Field quality in Electron Cooling Ring dipole.

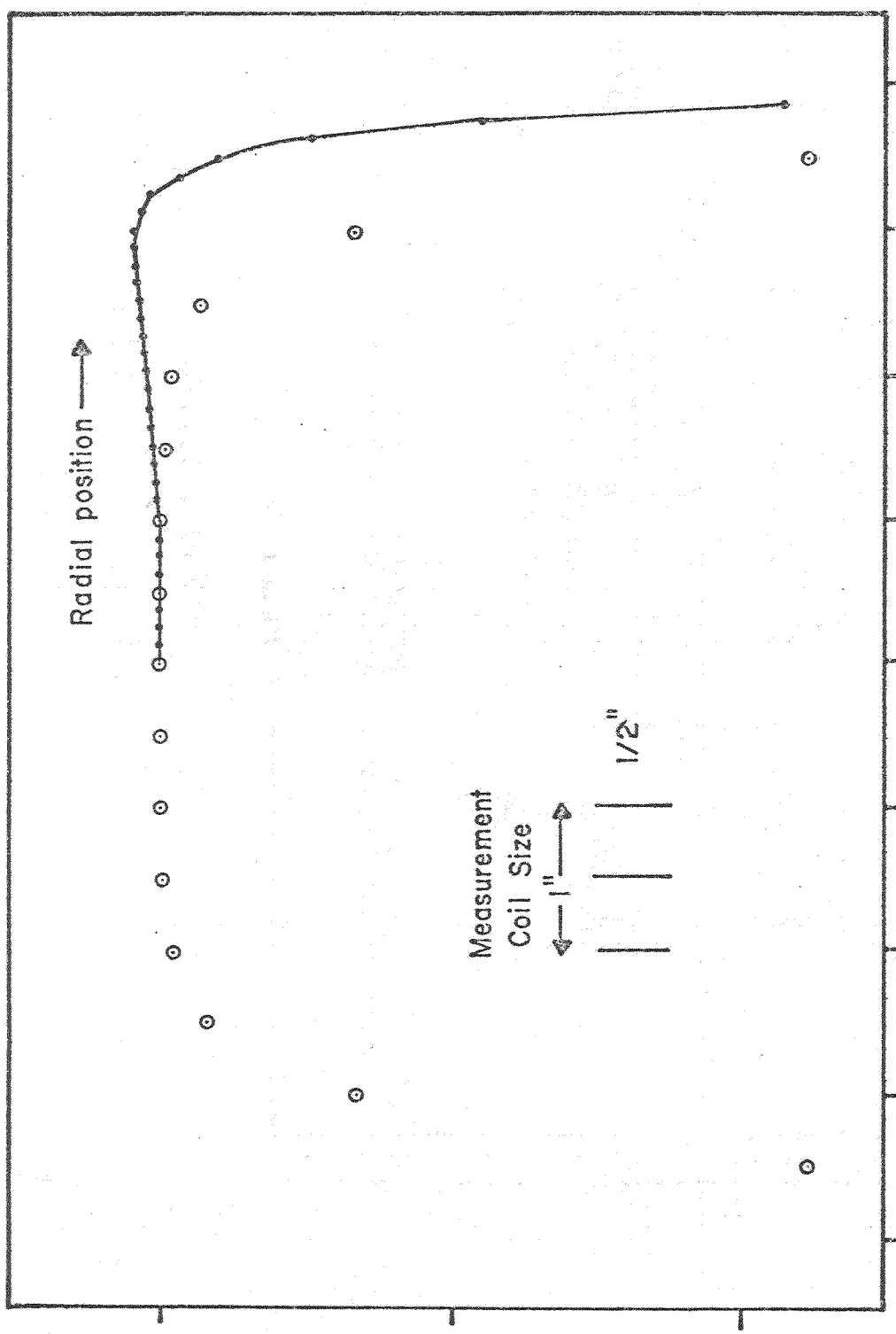

Fig. 5-4 Field quality in Electron Cooling Ring quadrupole.

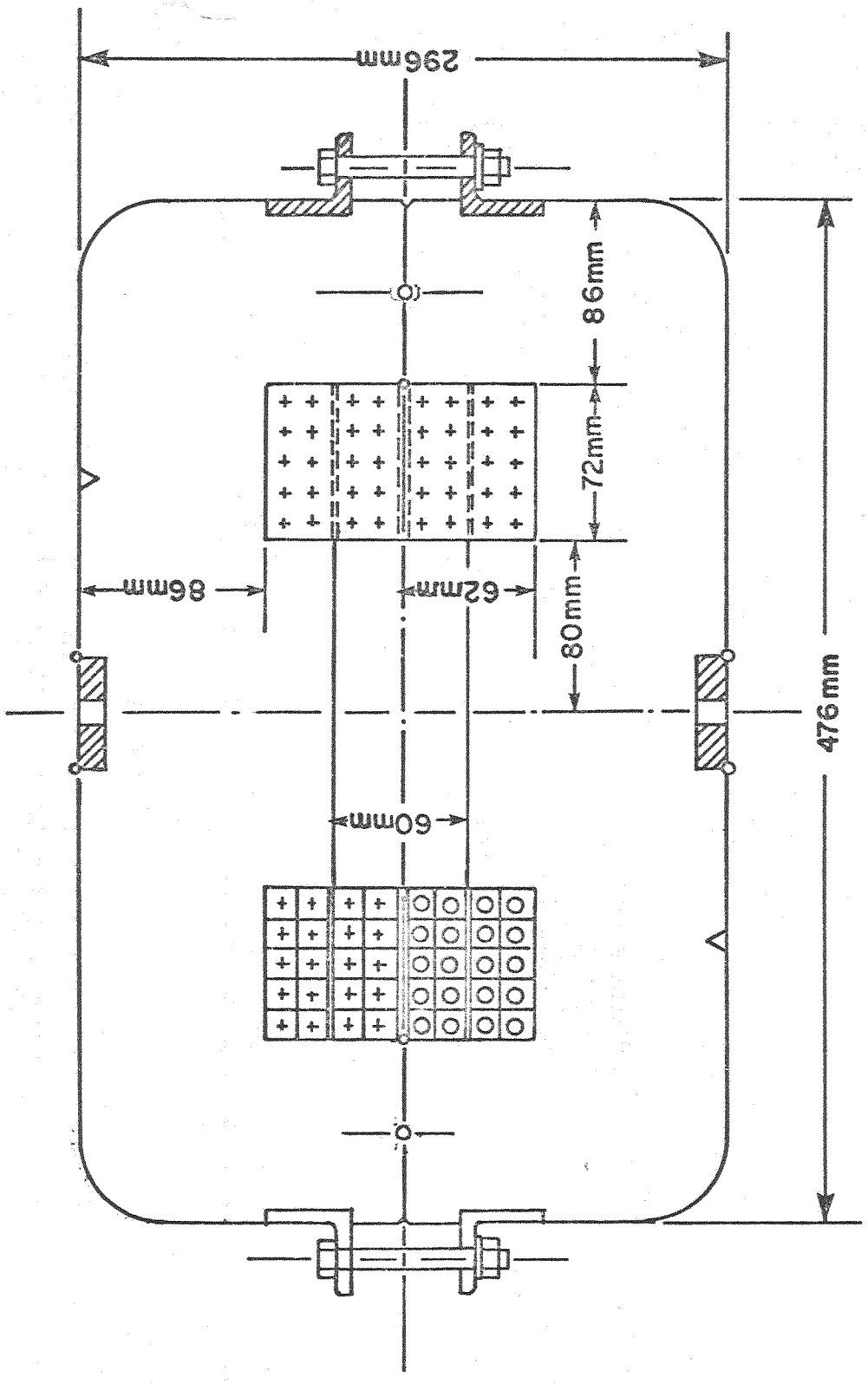

Fig. 5-5 Precooler dipoles.

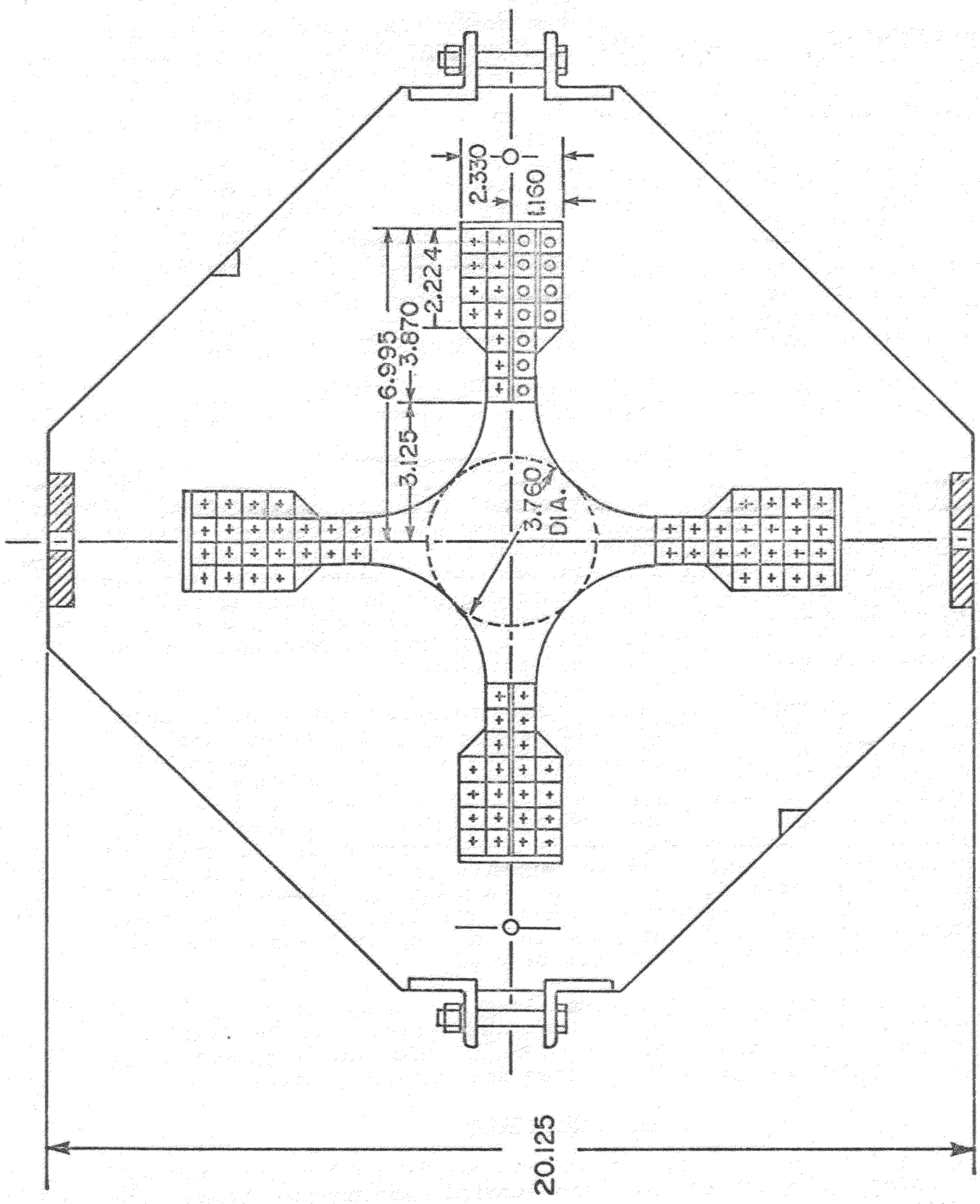

Fig. 5-6 Precooler quadrupole.

5.5 Vacuum System

The Precooler vacuum system design is based on a suitable modification of the existing Electron Cooling Ring system. Because of the magnetic cycle of the bending magnets, distributed ion pumping is not applicable. Thus the design is based on lumped commercial ion pumps in an all-metal, stainless-steel, welded system. Since the suggested average pressure of 2×10^{-9} Torr is higher than in the Electron Cooling Ring (10^{-10} T), pumping and baking requirements are relaxed. Two hundred 60 ℓ/sec ion pumps distributed around the ring with a nominal spacing of 2 meters will provide sufficient pumping capacity. A bake temperature of 200°C should provide a factor of 200 decrease in pressure (4×10^{-8} Torr unbaked to 2×10^{-9} Torr baked). The chambers are to be standard stainless tubing approximately 5-in. diameter for quadrupole and straight sections. The dipole chambers are rectangular in cross section and welded along the sides.

Basic degreasing followed by a 900°C, 10^{-5} Torr vacuum degas of chamber components is required prior to welding and assembly.

5.6 Controls and Diagnostics

The Precooler will employ normal Fermilab control hardware and software. Consoles employ keyboard and knob control, with an alphanumeric scope and storage scope for graphics. The consoles are serviced by Xerox 530 computers, which communicate with the equipment via Lockheed MAC-16 minicomputers and serial CAMAC. 1-MHz and 10-MHz clocks are synchronized with clocks in the whole facility. As the Fermilab control system is upgraded in the future, this system will also be upgraded.

The Precooler requires both routine and exotic beam-diagnostic equipment. The routine equipment for tuneup can utilize infrequent pulses of protons from the Electron Cooling Ring and can therefore be of low sensitivity. This includes 16 horizontal and 16 vertical position electrodes. Tune measurement can be by these same electrodes, which can also be used to tune out injection steering errors. A fast Q-electrode can be used for measurement of momentum spread, synchrotron frequency and injection phase error. Profile monitors can probably employ residual gas, in view of the modest vacuum requirements of the ring, although atomic jets, similar to the one developed for the Electron Cooling Ring might also be used.

More sophisticated diagnostics are associated with the stochastic cooling system. These diagnostics will be developed along with that system, but it is clear that they will certainly include high-gain wideband position and current probes.

5.7 RF Systems

The requirements for antiproton cooling and deceleration and for later acceleration of the cooled antiproton beams are

different enough that separate rf systems have been designed for these two functions.

5.7.1 Precooler Decelerating System. Deceleration in the Precooler will be done at h = 1, with a required frequency range of 385-628 kHz. The maximum voltage requirement, 65 kV, occurs at the end of the first deceleration period, where a 67.3 eV-sec beam is barely contained within a 72.9 eV-sec bucket. A higher upper-frequency requirement is set to accomodate injection into the Electron Cooling Ring at h = 2 if necessary. At this point, the system must be capable of generating 15 kV at 716 kHz.

The system can be composed of five separate cells of ferrite rings, each containing 44 rings, 18 cm i.d. × 45 cm o.d. × 2.5 cm thickness. An acceleration gap at the center of each cell will be driven push-pull by a pair of 10-kW tubes each capable of delivering an rf voltage swing of ±7 kV. The total ferrite volume per cell will be 1.47×10^5 cm^3 and the ferrite will be operated at an average rf flux level of 250 G (0.025 W/m^2). At this flux level at 600 kHz, the dissipation will be about 100 mW/cc or 14.7 kW. The two driver tubes, operating below 50% efficiency, will dissipate another 16 kW, making the total power per cell 30 kW. Each pair of tubes will be driven by a transformer-coupled solid-state driver.

The ferrite rings proposed are produced by TDK and are similar to those presently being tested for the ISABELLE rf accelerating system.

5.7.2 Precooler Acceleration System. We assume that the momentum spread ($\Delta p/p$) of the stacked beam in the Electron Cooling Ring can be maintained at about 10^{-4}. The energy spread is 73 keV and the longitudinal emittance is 0.06 eV-sec. The cooled stacked beam is to be bunched adiabatically at harmonic number 12, 15.032 MHz. The rf period is 66.5 μsec and if the beam is bunched to a bunch length of 35 μsec, then a period of 31 μsec will exist between bunches to allow for kicker rise and fall times. Because of the very small initial momentum spread, allowance is made for a factor of two emittance blow-up, resulting in an emittance of 0.01 eV-sec per bunch. An rf voltage of about 2 kV will provide the required bunching. This voltage can be provided easily by the surplus PPA rf cavity presently installed in the Electron Cooling Ring.

After bunching the bunches will be extracted individually into stationary buckets in the Precooler ring. The accelerating rf system in the Precooler will operate at harmonic number 21 so the rf frequency at 200 MeV will be 7.516 MHz, exactly half that of the Electron Cooling Ring. In order for the Precooler bucket shape to match the extracted bunches the required rf voltage in the Precooler will be 12.3 kV. The Precooler stationary bucket area at this voltage will be 0.076 eV-sec and the bucket to bunch area ratio is 7.6. Acceleration to 8 GeV in 5 seconds requires an initial accelerating voltage of 4.36 kV per turn, which can be

generated by a synchronous phase angle of 25.8°. If the beam is moved to this phase angle without increasing the rf voltage, the bucket area is reduced to 0.027 eV-sec and the beam will occupy about 37% of the bucket area. As the beam is accelerated, the rf voltage requirements will diminish, so the 10 to 15 kV required at the beginning of acceleration will be the maximum requirement anywhere. During the subsequent acceleration to 8 GeV, the Precooler frequency must be increased from 7.516 MHz to 13.193 MHz. The modest rf voltage requirement and frequency range are very well matched to the capabilities of a second existing surplus PPA rf cavity.

The Precooler harmonic number, 21, is an integral factor of the Main-Ring harmonic number, 1113 = (21 × 53), so that the Precooler frequency can be phase-locked to the Main-Ring injection frequency at 8 GeV. The Main-Ring frequency is precisely four times the Precooler frequency, so that the center of every fourth Main-Ring bucket can be made to overlap a Precooler bucket. If an additional factor of three longitudinal emittance blowup occurs during acceleration, so that each bunch has phase area 0.03 eV-sec, operation of the Precooler at 10 kV will result in a bunch length of 3.4 nsec. Bunches of this shape are well matched to stationary Main-Ring buckets with area 0.65 eV-sec. The required Main-Ring buckets are generated with a ring voltage of 1.2 MV, which is the normal injection voltage.

After appropriate bunching and phase-locking, bunches will be extracted from the Precooler and placed in the Main-Ring buckets at the desired locations. One Precooler acceleration cycle will be required for each of the twelve $\bar{p}$ bunches.

6. ACCELERATION AND STORAGE IN THE MAIN RING AND SUPERCONDUCTING RING

6.1. Bunch Reconfiguration in the Main Ring

In order to achieve the desired luminosity with antiproton-proton colliding beams, it is necessary to rebunch the proton beam in the Main Ring to approximately 12 bunches, concentrating more protons per bunch.

The plan is to debunch the beam from the usual harmonic h = 1113 by reducing the rf voltage adiabatically, then turning on a low-harmonic cavity to relocate bunches in phase space. After one-fourth of a phase oscillation, the bunches will have roughly clustered in phase at the lower harmonic, with an increase in total energy spread. The bunches are then recaptured in h = 1113 buckets by turning on the ordinary rf system.

Recent storage studies in the Main Ring have indicated, at an intensity of 2×10^{13} protons in approximately 1066 of the 1113 buckets, some 90% of the beam is contained within bunches 3 nsec long and appear to be matched to stationary buckets of 1.25 MV/turn. This corresponds to a bunch length $\Delta\phi$ of 0.5 radians and a bunch area of 0.19 eV-sec per bucket.

If the rf voltage is reduced until the bucket area has shrunk to the bunch area, then turned off, dilution by a factor $\pi/2$ will occur, so that the debunched emittance will be 0.3 eV-sec per bunch, corresponding to an energy spread of ±7.8 MeV or a phase-space density of 5.7×10^{10} protons/eV-sec. In order to create bunches containing 10^{11} protons, a charge bunch occupying area 1.75 eV-sec must be captured. To compensate for losses in extraction, injection, and acceleration, we take this area to be 2 eV-sec.

The voltage to create a 150-GeV, 2-eV-sec bucket at h = 1113 is 226 kV, so that recapture will create no problems. The maximum energy spread corresponding to a 2-eV-sec bucket is ±83 MeV, well within the observed useful momentum aperture at 150 GeV.

The low-harmonic cavity should keep the center of charge stationary with respect to h = 1113 buckets while rotating a set of bunches. Its harmonic number must therefore be a factor of 1113. Consider, for example, h = 21, corresponding to a frequency of 1.0019 MHz. This bucket covers the azimuthal region occupied by 53 bunches. Approximately 26 bunches can be rotated into a vertical strip 19 nsec long using a voltage of 12.7 kV. The synchrotron period is 0.6 sec, so rotation will require 150 msec.

If the same exercise is carried out at h = 53, f = 2.53 MHz, each bucket will encompass 21 of the original bunches. The required voltage is 32 kV, a little high. The problem of aligning the h = 1113 bunches vertically in this phase space also

appears to be more difficult than at h = 21, because of synchrotron tune spread, so the h = 53 option looks less favorable.

There are some questions as to how beam lifetime, instability, and emittance growth are affected in such an operating mode. CERN has recently reported[1] successful operation of the SPS at densities of 10^{11}/bunch, and instability was indeed noted. It may be necessary to include a high-frequency Landau-cavity system to maintain stability of such bunches.

Following this bunch reconfiguration the beam will be transferred to the superconducting ring in the normal direction.

6.2 Acceleration of p and $\bar{p}$ in the 1000-GeV Ring.

The acceleration system of the Superconducting Ring[2] is designed with 6 cavities. For bilateral acceleration and subsequent storage of protons and antiprotons, some restrictions must be imposed upon cavity spacing. By appropriate spacing and phasing of the rf fields in individual cavities, some aspects of bilateral operation can be optimized. The requirements of $\bar{p}p$ operation are:

(i) The rf system must create sufficient bucket area for simulataneous bilateral acceleration and storage of protons and antiprotons. Because the total number and longitudinal emittance of protons and antiprotons will almost certainly be quite different, the required bucket areas will not necessarily be the same.

(ii) The rf system should provide the capability for moving the bunch collision point azimuthally over some reasonable range (of order 20 m).

(iii) The system may be required to allow for independent control of the phase and amplitude (bucket location and size) of the proton and antiproton buckets.

If the requirement (iii) is satisfied, then (ii) is automatically, but it is possible that (ii) may be satisfied in a system that does not meet (iii).

Let us consider the cavity spacing required to satisfy the requirements listed above for bilateral acceleration. The basic unit is two adjacent cavities placed such that their effective gaps are $3\lambda/4$ apart, where λ is the rf wavelength. A particle moving downstream arrives at the second gap at a time phase $3\pi/2$ radians later than its arrival at the upstream gap. If the downstream-cavity gap voltage leads the upstream voltage by $\pi/2$, a particle moving downstream will see the gap voltages exactly in phase (modulo 2π), and consequently the two cavities provide maximum voltage and bucket area for such a particle. But a particle moving upstream will see the gap voltages exactly out of phase, and if the gap voltages are equal, will see no net

voltage. An additional similarly spaced doublet, with opposite relative phasing, can be placed arbitrarily close to the first pair. There is good reason to space the gaps of the nearest neighbors of adjacent doublets $\lambda/2$ apart so a pair of doublets (four cavities) will occupy a space of approximately 2.5 λ. All three requirements above can be satisfied through the use of such doublets. Upstream and downstream doublets can be driven from separate rf sources and operated at different amplitudes and phases.

As an example, Fig. 6-1 shows three doublets, the two outside doublets providing proton bucket area while the center doublet provides antiproton bucket area. A simple fanout system is shown to demonstrate that the required phasing can be accomplished using easily available components, quadrature hybrid junctions, and π radians splitters. In the array shown, with all gap voltages equal, the proton bucket area will be larger than the antiproton area by a factor of 1.414 during beam storage. During acceleration, the bucket-area difference will be slightly larger because the antiprotons will require a larger synchronous phase angle, because less voltage is available and consequently the moving-bucket factor reduction will be larger.

The cavity spacing described is essentially a series of cavities (1, 4 and 5) with their gaps spaced an integral number of half-wavelengths apart and another group (2, 3 and 6) with the same relative spacing, but all displaced by $\lambda/4$. Such an array of cavities can be phased in a slightly different manner to provide a greater <u>total</u> bilateral bucket area if requirement (iii) is relinquished. Such a phasing scheme is shown in Fig. 6-2. The proton and antiproton bucket areas are equal and each effective voltage is $0.707\ V_{tot}$.

With the phasing shown in Fig. 6-2, the intersection point is $\lambda/8$ to the left of the midpoint of the array. If the voltages of cavities 2,3 and 6 are reduced to zero, the intersection point will move to the midpoint of the array, with a slight reduction in bucket area, and if cavities 2, 3 and 6 are raised to maximum voltage with opposite phase, the intersection point will move to a point $\lambda/8$ to the right of the midpoint.

It is possible that the phasing of Fig. 6-2 could be used during acceleration and the phasing switched to the phasing of Fig. 6-1 to provide orthogonal control after storage energy is reached. Because of the quite different geometry of the two fanout systems, this phase switching would be difficult and would require great care to avoid phase-space dilution or loss of particles.

References

[1] D. Boussard et al., 1979 Particle Accelerator Conference, IEEE Trans. **NS-26**, NO. 3, June 1979, p. 3484.

[2] Fermilab staff, A. Report on the Design of the Fermi National Accelerator Laboratory Superconducting Accelerator, May 1979.

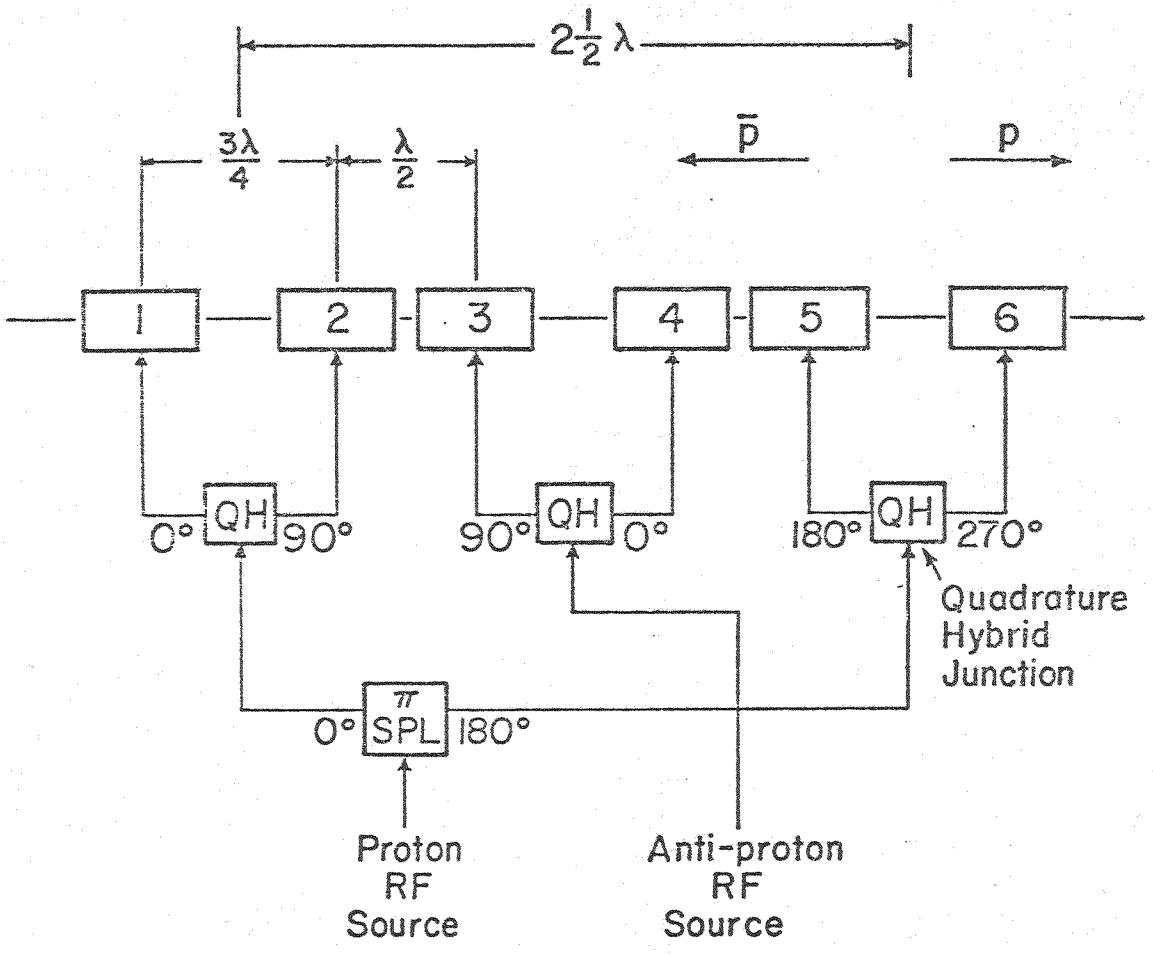

Fig. 6-1 Rf cavity spacing and phasing with orthogonal p̄p control.

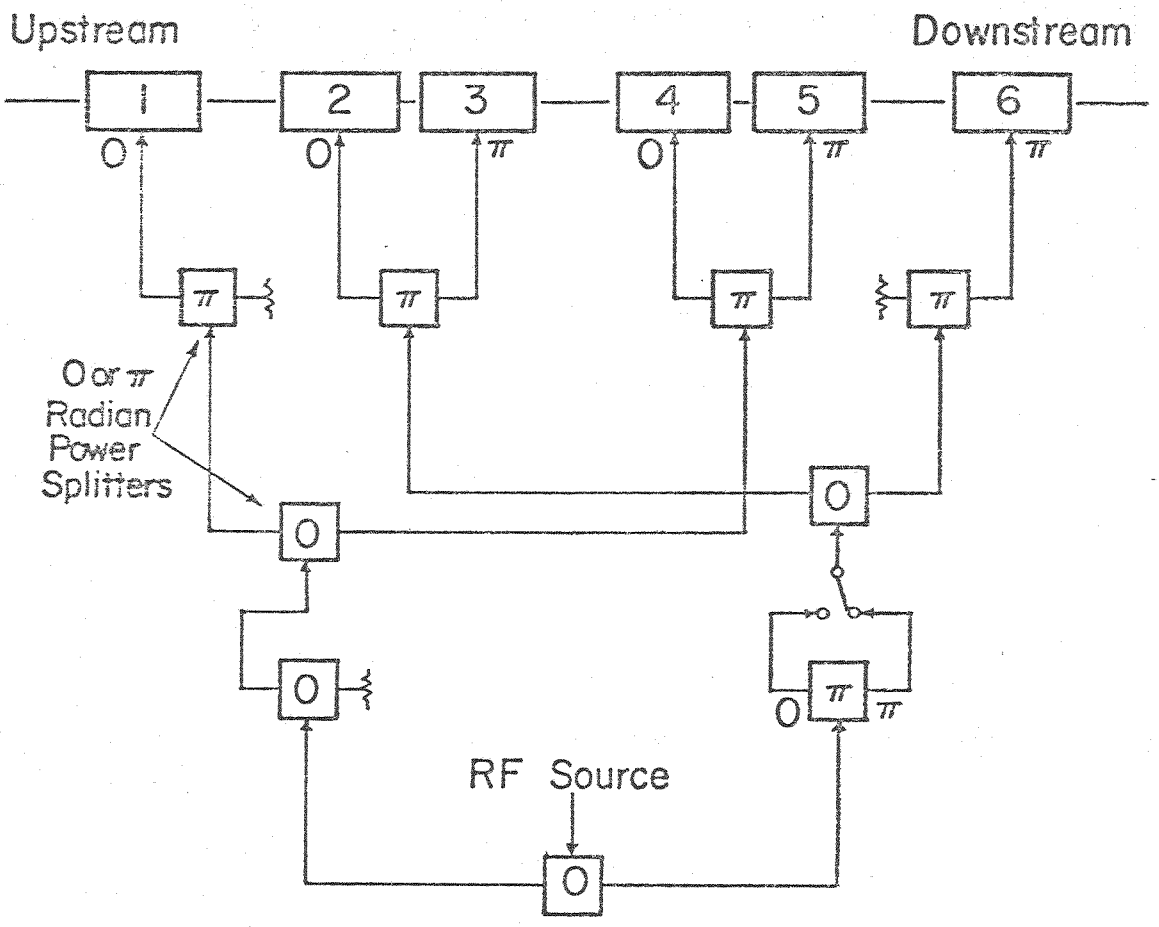

Fig. 6-2 Rf cavity spacing
and phasing without orthogonal $\bar{p}p$ control.

7. SHIELDING AND CONVENTIONAL FACILTIES

7.1 Shielding

There are two points along the sequence of the antiproton source that determine the shielding. The largest possible losses will occur either in the initial production of antiprotons in the Target Vault or in the acceleration of the accumulated antiproton beam to 8 GeV in the Precooler.

7.1.1 Target Vault. The production target is somewhat like the target areas in Fermilab external beams and will be shielded like them. The beam and target are 18 ft below grade. Components in the Target Vault will be radiation-hardened and provision will be made for removal of defective components by means of removable steel shielding. Estimates using a cascade Monte Carlo program, indicate that π^- and K^- are produced in the target in the broad momentum and angular range of interest at a ratio of 200 to 1, compared with the desired antiprotons. The negative secondaries not in the desired longitudinal and transverse phase-space interval will be selected out in the antiproton transport line to the Precooler (Sec. 3.9) and collimation will be provided to absorb the separated particles.

The π's and K's in the desired phase space will be injected into the Precooler together with the antiprotons and will decay while circulating. Approximately 90% of these particles are pions, which decay into leptons that do not interact strongly. The kaons are only 10% of the total and their decay products are at lower energy, so the shielding provided for 8-GeV antiprotons will be ample.

7.1.2 Precooler Ring. The circulating intensity of the accumulated 8 GeV beam of 10^{11} antiprotons in the Precooler is an order of magnitude less than the circulating proton intensity in the Booster. In addition, the average rate is much lower, because the Precooler has the beam only once in 5 hrs, rather than 15 times per second, as in the Booster. Shielding of 1 ft of concrete plus 2 ft of earth, compared with 5 ft in the Booster, is adequate for distributed losses. A rough simulation shows that it is also adequate for loss in a single magnet. The simulation gives an integrated dose of 20 mrem at the surface if 10^{11} antiprotons are lost in a single magnet.

7.2 Conventional Facilities

Antiproton Hall and the Target Vault were discussed in Sec. 3.3. Here we confine our discussion to the Precooler buildings.

7.2.1 Tunnel. A tunnel section is shown in Fig. 7-1. A clear space of 10 ft horizontally and 7 ft vertically is planned. Beam center line will be 3 ft above floor level and 18 in. in from the outer-radius wall. It is expected that the tunnel will be made of precast sections on a slab, a form that Fermilab has used

successfully in several recent applications. Reinforcing will be supplied where Kautz Road is to be rebuilt over the tunnel. Ventilation will be provided by fans.

7.2.2 Service Buildings. At the north, west, and south long straight sections, there will be 200 sq. ft service buildings at grade level with penetrations for electronic cabling. These buildings will be of conventional concrete-block construction, with conventional Fermilab coloring. Electrical service will be provided underground.

7.2.2 Main Building. The south long straight section will be covered by a 200 ft by 30 ft building for assembly, installation, injection and extraction. This building will be largely below grade level and reinforced concrete construction is appropriate and economical. Local shielding will be utilized as needed.

There will be a 10 ft covered loading area running the length of the building at grade level. Power supplies will be located in this area.

These facilities are shown in cross section in Fig. 7-2.

7.2.4 Utilities.

Electrical Service. There is enough spare capacity in the linac electrical system and an empty feeder running through the Booster pond to a point close to the Precooler site. Heating will be electric to avoid bringing gas service to the site.

Cooling Water. There is enough spare capacity in the Central Utility Building and an 8 in. pipeline close to the Precooler site.

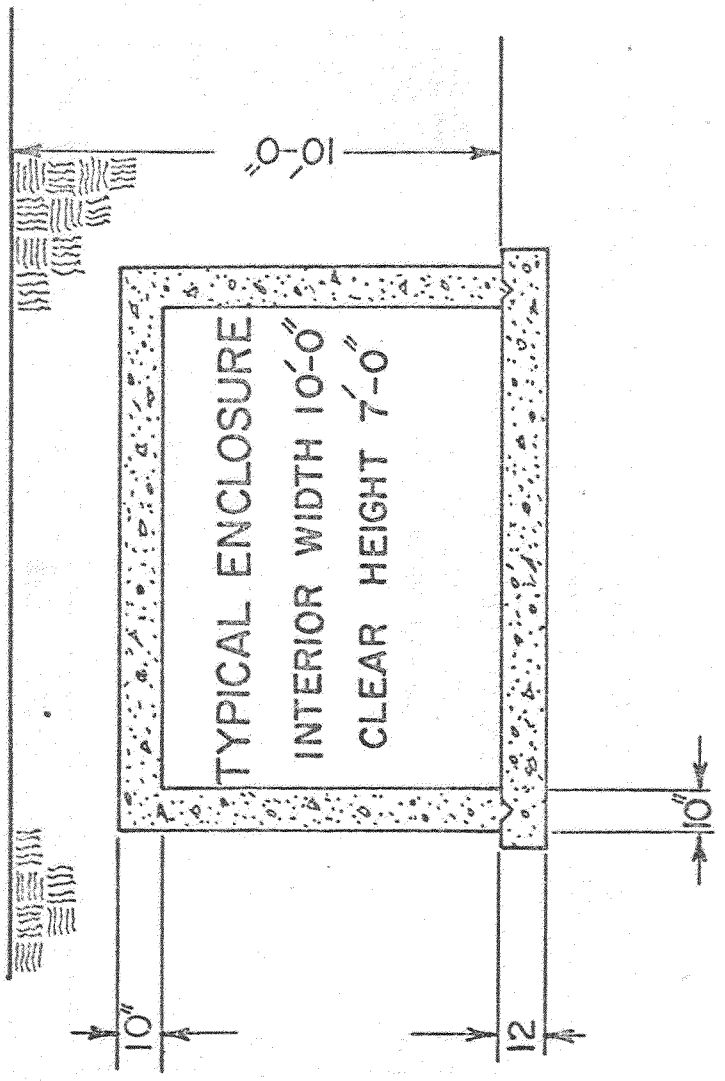

RING SECTION

Fig. 7-1

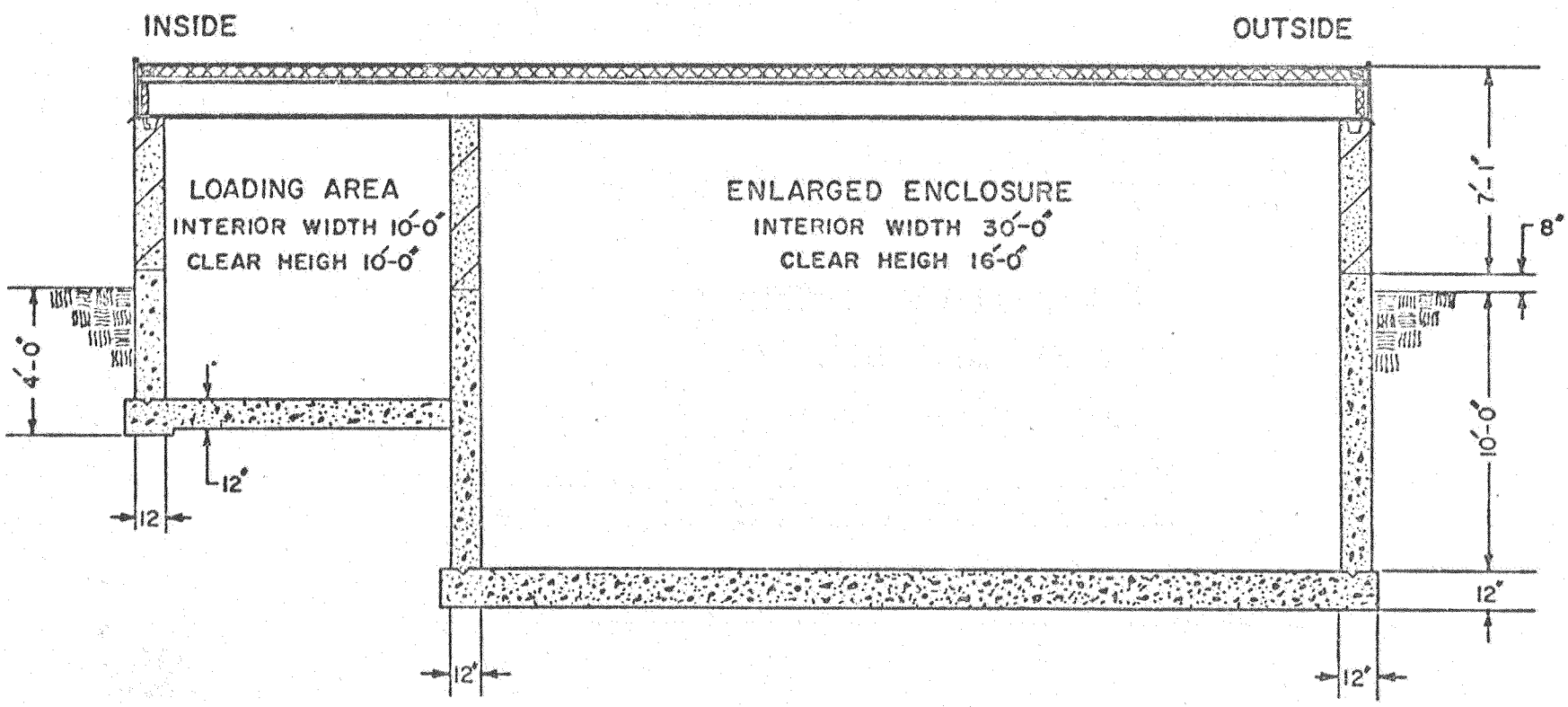

MAIN BUILDING SECTION

Fig. 7-2